# Effects of Discreteness in Solitonic Excitations:A Future Challenge or just Numerical Observations ?

P. Kevrekidis
*Department of Physics and Astronomy , Rutgers University*

December 7, 2001

**Abstract**

In this study we will focus on the significant effects of discreteness in solitons as they appear in a number of physical applications (material dislocations , charge density waves fluxons in arrays of Josephson junctions and many others). We will primarily be interested in the discrete version of the Sine-Gordon equation and on the kink and breather-like solutions of it (however we will give extensions of our results to other systems such as the $\phi^4$ or the double sine-Gordon (DSG)).Numerical Results will be presented that will explicitly demonstrate the vital role of discreteness in altering the continuum-like picture and in producing entirely new features in the problem such as internal shape modes of the solutions , pinning due to the Peierls-Nabarro barrier , emission of radiation or Brownian motion of the kink when driven by the fluctuations.We will also attempt to investigate the stability of these structures (kinks and breathers) using the Evans functions and Nyquist Theory techniques as well as to trace the very rich dynamics of the interactions of such structures (i.e. k-k or k-$\bar{k}$ interactions as well as breather-breather or breather-image collisions). In view of the dramatic effects of discreteness in the continuum description we are going to introduce an appropriate technique for discretizing continuum systems for computational purposes.Whenever possible the results of our numerical simulations will be compared with the relevant existing theories.

## 1 Introduction

After the pioneering work of N. Zabusky and M. Kruskal ([1]-[2]) in the 1960's the subject of nonlinear topological excitations has received an increasing amount of attention. The reason for that lies in the fact that for a number of generations of physicists the attempt to linearize a physical problem and do perturbation expansions around the linear behavior was the way to tackle even highly non-linear problems.However the existence of such structures such as kinks and breathers and their determination as exact solutions of these highly non-linear partial differential equations developed a whole new field of perturbing around these solutions and getting good results for the resulting linear excitations around these exact solutions.

In this paper ,as mentioned above , we will primarily consider these two types of solitonic excitations : kinks & breathers.Kinks are essentially heteroclinic connections (i.e. front-type solutions) whereas breathers are exponentially localised in space and periodically oscillating in time structures.

These two types of solutions are of increasing interest over the last decades since they appear to be a good model for a number of physical systems.One such example is the dynamics of magnetic flux propagation in Josephson junction transmission lines which are a promising way of transmitting,storing and processing information.The behavior of the magnetic flux can be modelled very efficiently by the kink propagation in the Sine-Gordon equation.

$$\phi_{tt} = \phi_{xx} - \sin\phi$$

(where subscripts denote partial derivative with respect to the subscript variable and $\phi$ is the magnetic flux).

Another intriguing application lies in the problem of charge density waves ([4]-[5]).The essence of the CDW phenomenon originates from the fact that in several quasi 1d conducting materials it is favorable under a certain T to undergo a phase transition to a state in which the electron density develops small periodic distortions which is followed by a modulation of the ion equilibrium positions.Hence a CDW condensate is formed which can be subsequently pinned by impurities or interchain coupling.Furthermore if its characteristic $\lambda$ has a commensurability relation with the lattice spacing then the motion of the CDW is occuring in a periodic commensurability potential. If we neglect the former pinning causes and we consider only this last one then the classical Hamiltonian of the system will be (see i.e [5]) : $H = \frac{n_c m^*}{N^2 {q_0}^2} \int dx (\frac{{\theta_t}^2}{2} + \frac{c_0 {\theta_x}^2}{2} + w^2(1-\cos\theta))$ where $n_c$ is the electron density, $m$ is the effective electron mass, $q_0$ is the wavelength of the undeformed condensate and $\theta = N\phi$ where $\phi$ is the phase of the fluctuations of the collective wavefunction of the condensate away from the equilibrium state.Thus a kink-type solution can be adequately used to model the behavior of the CDW condensate. These solitonic solutions seem to also have applications in biological problems: recent molecular dynamics ([7]-[9]) simulations have used the discrete sine-Gordon (which is the main subject of this paper) , quite successfully, as a simple model for the thermal denaturation of the DNA strand.These numerical experiments have provided valuable insight in the understanding of the denaturation problem (i.e. they suggest that kink-antikink pair collision is a necessary prior stage to the denaturation transition). A further host of numerous applications consists of the ferroelectric and ferromagnetic materials ([10-11]) in which the appearance of domain walls in one dimensional or quasi one dimensional systems is quite generic. A remarkable application of these types of models that we will address in this study is their use for the description of sub-nuclear particle properties which is in fact the area from which some of these model equations (i.e. the $\phi^4$ model equation : $\phi_{tt} = \phi_{xx} + \phi - \phi^3$ ) originated. Striking as it may seem these solitonic solutions have a number of symmetries such as momentum -in the continuum case- or topological charge -i.e. the number of kinks and antikinks in the problem is conserved- which can create a quite strong basis for a particle-soliton analogy which is of wide applicability in field theories. Last but certainly not least in this short list of systems triggering our numerical and theoretical studies, in terms of applications, is the problem of dislocations and their propagation in condensed matter systems.One can understand this analogy quite well by imagining these localised dislocation excitations either as nucleated as a result of stress or as i.e. emitted from a crack tip.These excitations, in their attempt to propagate through the lattice periodic substrate encounter a periodic potential referred to as Peierls-Nabarro potential in the classical dislocation theory (and by analogy as we will see the same name is used in the case of discrete solitons in a lattice).Thus the acceleration of these structures will be determined by the linear strain (i.e. gradient) potential term $\phi_{xx}$ as well as by the local periodic substrate potential.Hence, the Sine-Gordon equation seems to be a good model for this system as well. In general it is widely recognized that condensed matter physics (where most of the above mentioned applications, as well as others such as nonlinear spin waves, incommensurate systems or bond alternation domain walls in polyacetylene, appear) is a "storehouse" of solitons([5]).

However this last problem starts posing the vital role of discreteness in the model since the potential is on the periodic lattice and thus the system under study is inherently discrete.Furthermore the same is true for the CDW problem as well as for the the denaturation of the DNA strand since in that case one has to deal with a "lattice" of base pairs and the variable (in the discrete Sine-Gordon type of equation of the model) is the transverse stretching of the hydrogen bonds connecting the bases.

Soliton problems of models such as the Sine-Gordon equation ($u_{xx} + \sin u = u_{tt}$ arising from the potential $V = 1 - \cos u$) or the $\phi^4$ model ($u_{xx} + u - u^3 = u_{tt}$) or even the double Sine-Gordon (DSG: $u_{tt} = u_{xx} + \lambda \sin u + \sin 2u$ arising from $V[u] = \lambda(1-\cos(u)) + \frac{1}{2}(1-\cos(2u))$) have been extensively studied and have well-known charcteristics in the continuum case.However the above mentioned problems strongly suggest that it is important to acquire a deeper understanding of whether there are significant differences between the discrete and the continuum descriptions.The main aim of this work is to trace these differences and highlight the physical reasons causing them to occur.

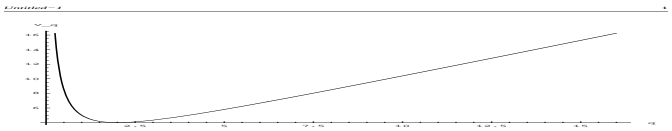

Figure 1: Wobbling Potential of Kink in 2-Parameter Continuum Variational Approach

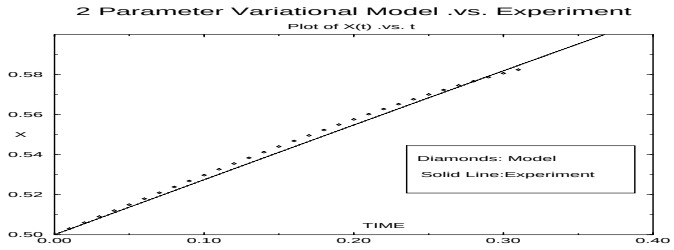


Figure 2: Comparison of 2 Parameter Variational Approach with Experiment

# 2 Single Kink Behavior

## 2.1 Continuum Description

The continuum Sine-Gordon belongs to the class of completely integrable Hamiltonian systems with an infinite number of invariants. Among them are the energy of the system $H = \int dx {y_t}^2/2 + {y_x}^2/2 + (1 - \cos(y))$ , the momentum $p = \int dx(y_x y_t)$ and the topological charge $Q = \frac{1}{2\pi} \int y_x dx$ which can be readily seen to correspond to the to the number of kinks - the number of antikinks in the system (thus the analogy in particle systems with charge conservation in particle interactions).The well-known explicit solution to the equation is known to be in this case:

$$y = 4 \arctan \exp \left[\pm k(x - x_0 - vt)\right]$$

where the (-) corresponds to the antikink and $k = \frac{1}{\sqrt{1-v^2}}$.$X_0$ is the initial position of the kink and v is its velocity.One directly sees that this solution is constructed from the static kink solution ($v = 0$) by means of a Lorenz boost. This solution has an energy of $8/k$ and it basically constitutes an heteroclinic connection between the maxima of the potential energy $V$. The periodic nature of the potential renders clear the fact that this is a solution modulo $2\pi$.

Let us verify the fact that this ansatz (i.e. $y = \arctan(\exp y)$ ) yields a solution to the equation in a rather elaborate way :using the variational formulation.This will permit us to make a brief introduction to the techniques of the variational calculus (one good reference to which is [13]) which we are going to use further along the lines of this presentation.

## 2.2 Interlude I:Variational Techniques

Let us assume an ansatz $y = \arctan(k(t)(x - X(t)))$ as a solution to the equation $y_{tt} = y_{xx} + \frac{1}{d^2}\sin(y)$.Substituting this ansatz in the action functional S[y]:

$$S[y] = 8 \int dx \frac{1}{4\cosh k(x - X(t))^2} [(\dot{k}(x - X) - k\dot{X})^2 - k^2 - \frac{1}{d^2}]$$

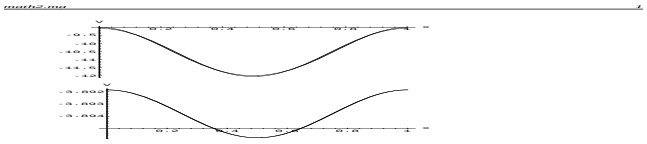

Figure 3: Peierls-Nabarro Potential Barrier in the 1 Parameter Variational Model and its Cosinusoidal Fit for Small d (0.3) and for large d (1.0)

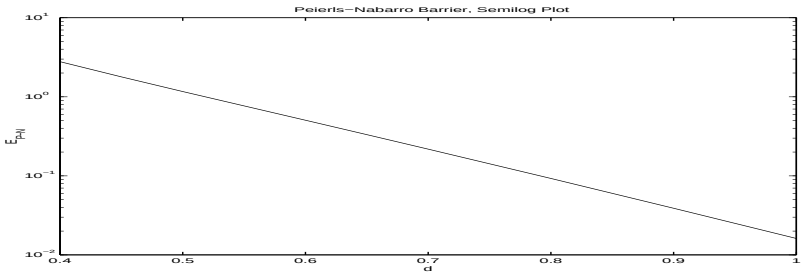


Figure 4: Semilog Plot of the P-N Well Depth as a function of the Discreteness Parameter d

Therefore making the substitution $\xi = k(x - X)$ and rendering thus the integrals dimensionless one obtains the equation : $S = \frac{\dot{k}^2}{k^3} S_1 + ((k\dot{x})^2 - k^2 - \frac{1}{d^2}) S_2$ (since the odd function integrals disappear) where $S_1 = \int_{-\infty}^{\infty} \frac{\xi^2}{(\cosh \xi)^2}$, $S_2 = \int_{-\infty}^{\infty} \frac{1}{(\cosh \xi)^2}$. Then one uses the Euler-Lagrange equations (since the action contains first order time derivatives only):

$$\frac{\partial L}{\partial x} = \frac{d}{dt} \frac{\partial L}{\partial \dot{x}}$$
$$\frac{\partial L}{\partial k} = \frac{d}{dt} \frac{\partial L}{\partial \dot{k}}$$

to obtain the following formulas (making also the change of variable $q = k^{\frac{5}{2}}$) $q^{\frac{2}{5}} \dot{X} = constant = C$

$$\ddot{q} = -\frac{\partial V}{\partial q}$$

where $V = \frac{c_2}{2c_1} (\frac{C^2 + \frac{1}{d^2}}{q^{5/2}} + q^{5/2})$ (a plot of V is given in figure [1] ). As one can see the minimum of the potential well corresponds to the case $k^2 = C^2 + \frac{1}{d^2}$ and $C = k\dot{X}$ which gives the familiar solitonic excitation kink solution of $\dot{X} = const. \Rightarrow x(t) = x_0 + vt$ and $k = \frac{\gamma}{d}$ However it seems puzzling that the variational formulation of the continuum problem seems to be giving the possibility for oscillations around this potential well minimum (as can be directly seen by the form of V). These solutions do not arise in the full nonlinear partial differential equation.In order to see that one can use the ansatz $y = 4 \arctan[\exp k(t)x + X(t)]$ naming $s = k(t)x + X(t)$. Then substituting in the PDE one obtains after some simple algebra the equation:

$$y_{ss}(\dot{k}^2 x^2 + 2\dot{k}\dot{X}x + \dot{X}^2 - k^2 + \frac{1}{d^2}) + y_s(\ddot{k}x + \ddot{X}) = 0$$

and taking the $x \to \infty$ limit since x should satisfy the equation at any spatial point one retrieves the equation $\dot{k} = 0$ which holds k and consequently X constants.Thus the point of this exercise is that one should be careful in using the variational formulation in terms of the physical meaning of the solution one gets. The resulting functional forms will be minima of the action but it should also be cross- checked that they are actual solutions of the PDE under study.

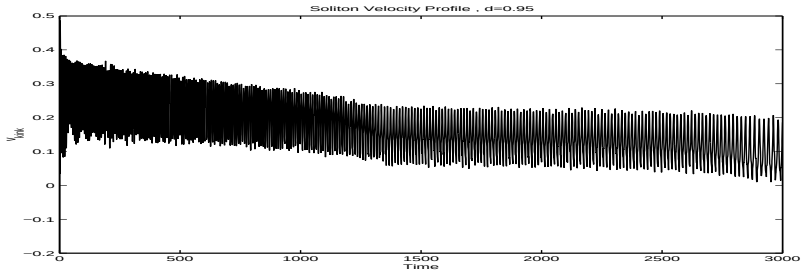


Figure 5: Kink Velocity Time Evolution ($v_0 = 0.3$)

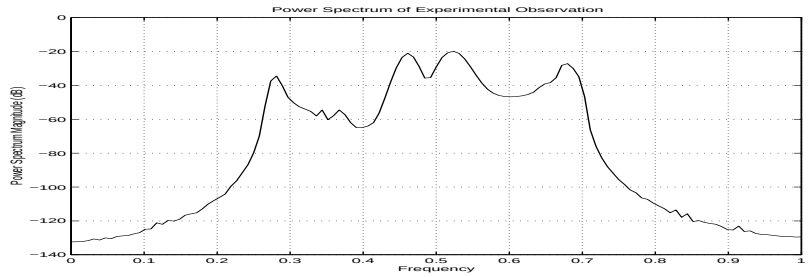


Figure 6: Power Spectrum Density of the Fluctuations (experiment)

It is amusing that a similar phenomenon had been observed as early as 1984 by Campbell , Schonfeld and Wingate in their seminal work on soliton collisions in the case of the $\phi^4$ model ([41]). There, the ansatz $\phi = \tanh \frac{y_0(t)(x-x_0(t))}{\sqrt{2}}$ admits an exact time-dependent solution: $y_0 = A/\dot{x_0}$ and $\dot{x_0} = \frac{a}{\sqrt{a^2+1}}(a + \sqrt{a^2-1}\sin(wt))$ with $w = \frac{1+a^2}{\beta}$. This solution would , if it existed in the case of the full PDE, correspond to a wobbling and translating isolated kink. However direct substitution of this ansatz to the PDE results in the conclusion that it cannot be an exact solution. The fact that the discrete kinks appear to be wobbling gives rise to the question of whether this solution can appear in the discrete case as well to the quest of its orgins in the continuum case. Clearly the question of why the action projects out a wobbling kink when it does not correspond to a solution of the full non-linear equation deserves further study.

So far we have set the stage of the continuum Sine- Gordon equation. Therefore we can now proceed to view the modifications that discreteness imposes on this picture.

From this point on we are going to focus our attention primarily to the discrete Sine-Gordon equation with occasional excursions to other models.

The discrete Sine-Gordon equation was first put forth by Frenkel and Kontorova in 1938 [14] as a model for the study of dislocation propagation. It consists of the substitutions of the second partial derivative in space of our familiar Sine-Gordon equation by the corresponding second difference in space (a 3-point finite-difference stensil).Therefore the equation reads:

$$y_{tt} = \Delta_2 y - \frac{1}{d^2}\sin y$$

where $\Delta_2 = \frac{y_{i+1}+y_{i-1}-2y_i}{h^2}$ where $h$ is the spatial discretization that from here on will be set to 1 lattice spacing as is done in the classic paper of Peyrard and Kruskal ([15]) on the subject.

Artificial as it may seem this system is not only particularly relevant to the discrete problems mentioned above but it also arises in very simple physical situations such as the elastically coupled torsion pendula.

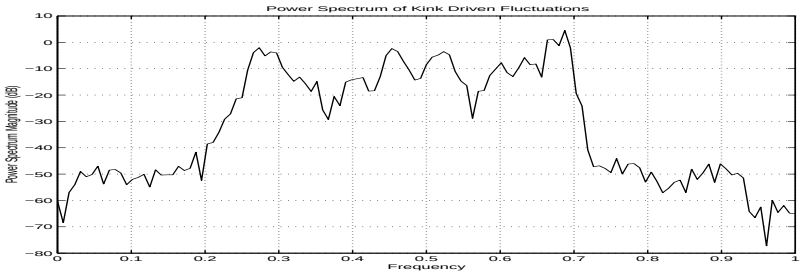


Figure 7: Power Spectrum Density of the Fluctuations (model)

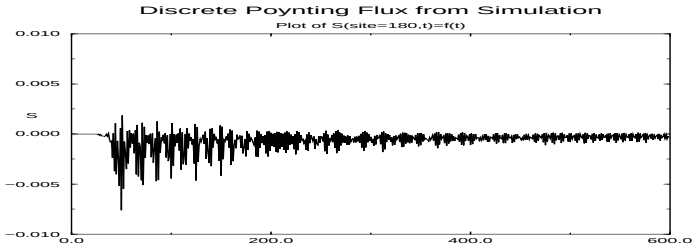


Figure 8: Poynting Flux Time Series for Site [180] (at the wake of the kink)

## 2.3 Discrete Description

In this case, the integrability of the system is lost and thus one no longer has exact static or propagating solutions of the system. Furthermore the kink solutions no longer have the same energy but there is a stable and an unstable kink configuration. As might be intuitively clear to the experienced reader there is one type of configuration with a lattice point in the center ($y = \pi$) of the $2\pi$ kink which is unstable (i.e. has a larger energy $E = \sum (\frac{{y_i}_t{}^2}{2} + \frac{(y_{i+1}-yi)^2}{2} + \frac{1}{d^2}(1-\cos y_i))$. Thus as the kink propagates through the lattice it oscillates between these two extrema in passing through the lattice points. Therefore discreteness gives rise to a potential barrier in which the kink oscillates. This is the so called Peierls-Nabarro barrier which is analogous analogous to the one the dislocations have to surpass in order to move by one lattice spacing.

The existence of such a barrier has a major significance since it implies that if the kink does not have enough energy (i.e. small $v_0$), it will get pinned down by the lattice and will no longer propagate. Thus, discreteness can have a rather dramatic effect in the dynamics of the system and can for example forbid to bits of information in a discrete array of Josephson junctions to propagate and get transmitted.

Of course all the above phenomena are occurring in the case of small values of the discreteness parameter d (typical values for which discreteness effects are observable are $d \leq 1$.For large values of d one retrieves the familiar continuum limit behavior. In fact the Peierls-Nabarro barrier -evaluated as the $E_{unstable} - E_{stable}$ (where the subscripts correspond to the configurations mentioned above)- has been numerically found to decay as $\exp(-\pi^2 d)$ as d increases.

There has been a number of efforts to theoretically explain the behavior of the single kink in the discrete system (forgetting for the moment the radiative effects that will be considered in the next section). Our approach is based on the variational formulation presented above however modified now for the case of the discrete system.

Our ansatz for the solution will once again be : $y = 4\arctan[\exp k(t)(i - X(t))]$ which chooses the same spatial discretization as employed in our numerical simulations. Substituting this functional form in the action one gets:

$$S = \int dt \sum_i \frac{1}{4\cosh(k(i-X))^2}[(\dot{k}(i-X) - k\dot{X})^2 - \frac{1}{d^2}] -$$

$$(\arctan(\exp(k(i+1-X))) - \arctan(\exp(k(i-X))))^2$$

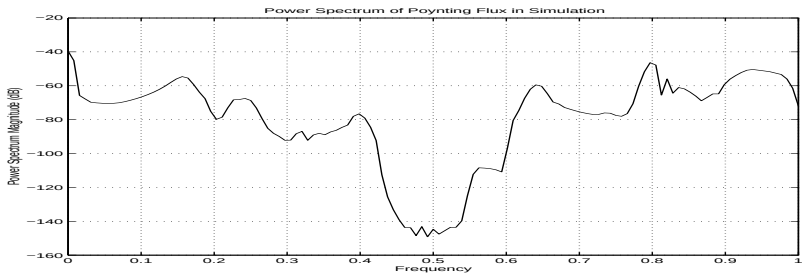


Figure 9: Power Spectrum Density of the Poynting Flux at Site [180] (model .vs. experiment)

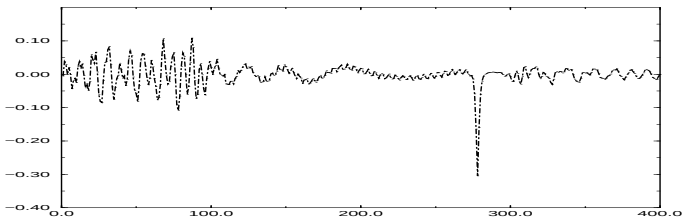

Figure 10: Velocity Profile of F-K Lattice Close to a Quasi-Steady State

Then using the Euler-Lagrange equations one obtains the following equations for the time evolution of the parameters k,X

$$\sum_i \frac{\sinh(k(i-X))}{2\cosh(k(i-X))^3}[(\dot{k}(i-X)-k\dot{X})^2+\frac{1}{d^2}](i-X)$$

$$=\sum_i \frac{\ddot{k}(i-X)-2\dot{k}\dot{X}-k\ddot{X}}{2\cosh(k(i-X))^2}(i-X)+$$

$$\sum_i(\arctan(\exp(k(i+1-X)))-\arctan(\exp(k(i-X))))(\frac{i+1-X}{\cosh(k(i+1-X))}-\frac{i-X}{\cosh(k(i-X))})$$

$$\sum_i \frac{sinh(k(i-X))}{2\cosh(k(i-X))^3}[(\dot{k}(i-X)-k\dot{X})^2+\frac{1}{d^2}]$$

$$=\sum_i \frac{\ddot{k}(i-X)-2\dot{k}\dot{X}-k\ddot{X}}{2\cosh(k(i-X))^2}+$$

$$\sum_i(\arctan(\exp(k(i+1-X)))-\arctan(\exp(k(i-X))))(\frac{1}{\cosh(k(i+1-X))}-\frac{1}{\cosh(k(i-X))})$$

One can use the energy conservation equation which is equivalent to a linear superposition of the above equations in order to acquire a simpler first order relation between k and X : $(\dot{k})^2S_7-2k\dot{k}S_6+S_1k^2(\dot{X})^2+\frac{S_1}{d^2}+2S_{10}=E$ where $S_1, S_6, S_7$ are k,X dependent sums. Using similar summation conventions for notational simplicity one can write the remaining second order equation as: $\ddot{k}S_7-2\dot{k}\dot{X}S_6-k\ddot{X}S_6=S_8-\dot{k}^2S_9+2k\dot{k}\dot{X}S_3-(k^2\dot{X}^2+\frac{1}{d^2})S_2$. One can then go on to solve the energy equation for $\dot{X}$ and can thus obtain the time evolution of both k and X by substituting the first and second time derivatives of X in the k-equation. The resulting equations then are (where $S_1$-$S_{10}$ are appropriately defined k,X dependent sums):

$$\dot{X}=\frac{B+\sqrt{B^2+4AC}}{2A}$$

$$\ddot{k}=\frac{(2\dot{k}\dot{X}S_6+S_8-\dot{k}^2S_9+2k\dot{k}\dot{x}S_3-((k\dot{X})^2+\frac{1}{d^2})S_2+kS_6\dot{B}_1/(2A_1))}{S_7-2k^2{S_6}^2/(2A_1)+(-4B_1(S_6k)^2+8A_1kS_6S_7\dot{k})}$$

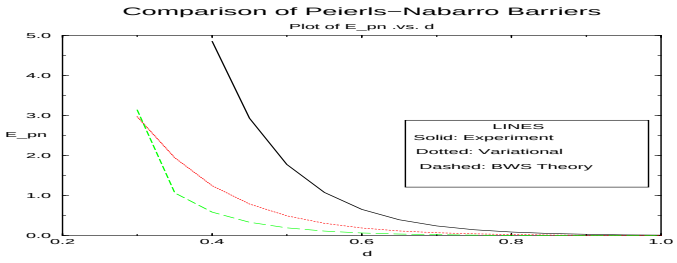


Figure 11: Comparison of Peierls-Nabarro Barriers (experiment .vs. BWS theory and variational approach)

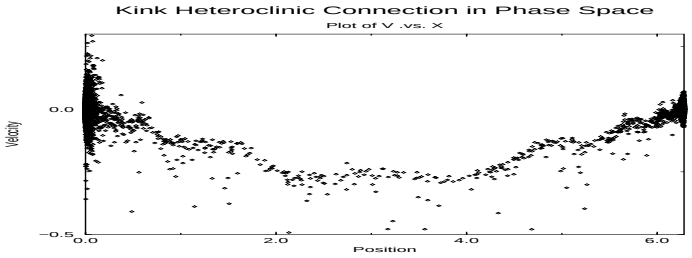


Figure 12: Kink Heteroclinic Connection Arising in Phase Space

$$\frac{-B_1\dot{A}_1/(2{A_1}^2) - \sqrt{}({B_1}^2 + 4A_1C_1)\dot{A}_1/(2{A_1}^2) + (2B_1\dot{B}_1 + 4\dot{A}_1C_1 + 4A_1\dot{C}_1)/(4A_1\sqrt{}({B_1}^2 + 4A_1C_1))}{S_7 - 2k^2{S_6}^2/(2A_1) + (-4B_1(S_6k)^2 + 8A_1kS_6S_7\dot{k})}$$

where $A = S_1k^2$ , $B = 2S_6k\dot{k}$ , $C = E - \frac{S_1}{d^2} - 2S_{10} - \dot{k}^2S_7$ and $\dot{B}_1 = \dot{B} - 2S_6k\ddot{k}$, $\dot{C}_1 = \dot{C} + 2\dot{k}\ddot{k}S_7$.

We attempted to numerically integrate these coupled ODE'S for the parameters k(t),X(t) and to compare our results with the results of the numerical integration of the discrete Sine-Gordon system.

Of course the Frenkel-Kontorova model with a single continuum kink form as its initial condition involves the appearance of radiation as we will see in the next paragraph.A typical figure of the space time evolution of a discrete F-K kink is given in the 3d figure [$3d_1$] (for reasons of convenience we will give all the 3 dimensional graphs -along with their captions- in the end of the text and thus they will have a separate enumeration than the rest of the graphs). However for sufficiently small velocities this effect is smaller and thus one can more efficiently compare the 2 parameter variational approach with the actual numerical experiment.

Let us, at this point, before getting into the details of this comparison, say a few words about the numerical integration scheme. The method of numerical integration is a fourth-order explicit Runge-Kutta scheme with a typical time-step of 0.01 (as in [15]).Damping was applied to the last 10 points on each side of our 400 point lattice on which the coupled ODE's of the F-K model were solved fixing the boundary conditions to $y_0 = 0$ , $y_{400} = 2\pi$ (the so called kink boundary conditions). The initial condition was a discretized version of the exact continuum solution with relatively small velocity ($v = 0.3$) and in the discreteness dominated regime of d ($d = 1.0$).

The results for the value of $X(t)$ .vs. time are given in figure [2].On can see that the 2-parameter variational model follows the numerical experiment closely for some time but the drop of speed is much faster than in the numerical simulation in which practically during the run the speed of the kink is unaltered. This quite abrupt drop of velocity to 0 in the 2 parameter variational model causes a numerical instability to set in and one is unable to further trace the theoretical predictions. However it seems already that even for small times the model prediction is not consistent with the experimental one. Thus one is led to doubt whether it is appropriate to use more than one parameters in the action variation (since the proper behavior is not retrieved even in the continuum). Another point which might be worth noticing is that the theoretical model seems to be oscillating for the period of time in which the energy is conserved. It might be interesting (although computationally cumbersome) to try to optimize the 2 parameter variational model code to see if indeed this oscillation is picking up the corresponding motion to the wobbling that the 2 parameter variational model seems to be yielding in the continuum case. We will address this

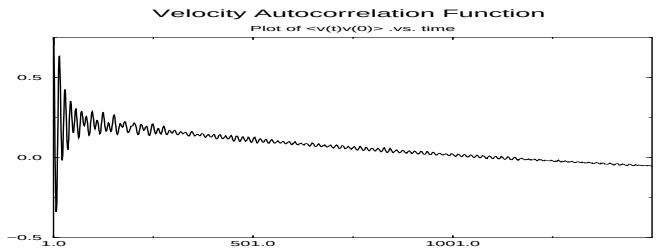


Figure 13: Autocorrelation Function of Kink's Velocity

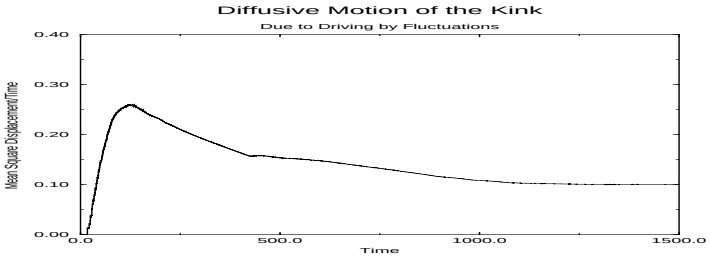


Figure 14: Mean Square Displacement of Kink over Time Plotted .vs. t

issue in more details in future studies.

Hence, we went on to consider the discrete variational one parameter model which seems to be the most natural implementation of the calculus of variations in the discrete system since for constant k it picks out essentially the energy equation. This can be seen directly from the variation equation with respect to X given above: In that equation, setting $k = const.$ and multiplying by k one can directly see that this is the total derivative of the energy

$$E = \sum \frac{1}{4\cosh(k(i-X))^2}[(k\dot{X})^2 + \frac{1}{d^2}] + (\arctan(\exp(k(i+1-X))) - \arctan(\exp(k(i-X))))^2$$

One can rewrite this conservation law as $\frac{M}{2}\dot{X}^2 + V = E$ where $M$ is defined as $M = \sum \frac{k^2}{4\cosh(k(i-X))^2}$ and V is the potential term. Then $\dot{X}^2/2 = -V_{eff}$ where $V_{eff} = -\frac{E-V}{M}$ and thus $\ddot{X} = -\frac{\partial V_{eff}}{\partial X}$.One can actually plot this effective potential. Its shape can be quite well approximated by a cosine curve as can be seen in figure [3] (with increasing accuracy in the approximation for higher values of d) and from the depth of the well we can estimate and plot the Peierls-Nabarro barrier for our model which is shown in a semilog plot .vs. d in figure [4].We can see that this model captures the exponential decay of the barrier with increasing d and thus is qualitatively correct however the exponent is $\simeq 8.65 \pm 0.2$ which is quantitatively different than the numerical prediction of slope $-\pi^2$. Therefore our one parameter variational model is the most appropriate approach (also in comparison with other theories that will be introduced and compared to it in the next subsection).However one should not expect to capture the full wealth of the behavior of the discrete Sine- Gordon model by means of a simple one collective variable approach.

## 2.4 Radiation Effects

One of the first things one notices in the numerical simulations of the system is the fact that apart from the propagating kink in the discrete system there are also radiative effects which appear both in the wake as well as in front of the kink. Of course some of these effects are an outcome of the fact that the initial condition of the continuum constant speed kink solution profile is not an exact solution for the discrete case.Therefore the kink tends to adjust its velocity and its shape so that it can more easily propagate through the discrete lattice. Obviously this is quite different than the case of continuum solitons where such effects are absent. However, the numerical experiments indicate that the kink radiates even at later times as it propagates through the lattice.In order to explain these

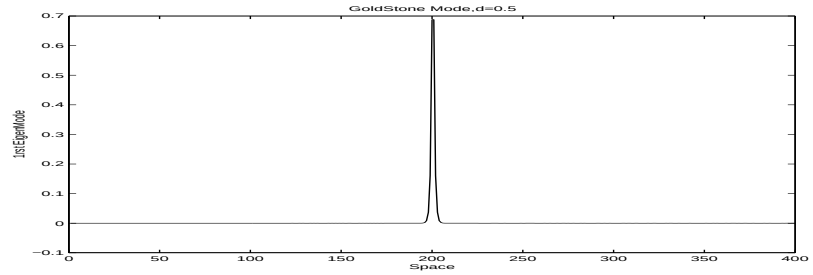


Figure 15: GoldStone mode in the Discrete F-K Model

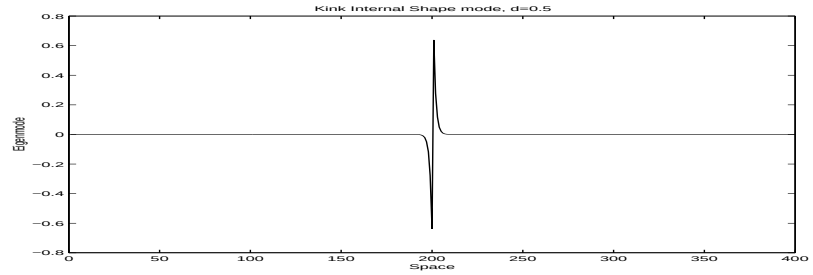


Figure 16: Localized Shape Mode Arising Due to Discreteness in the F-K Lattice

radiative effects Peyrard and Kruskal introduced a simple model that however maintains the characteristic effects of discreteness and thus they were able to capture the main qualitative and some quantitative aspects of the problem.

Removing the kink from the equations of motion and incorporating its effect as a driving force $f_i = \frac{d^2}{dt^2} y_{kink}(i,t)$ where $y_{kink}$ is the function describing the kink shape (i.e. the discretized version of a continuum kink solution) they obtained an equation for the fluctuations $u_i$:

$$\ddot{u_i} = \Delta_2 u_i - \frac{1}{d^2} u_i + f_i$$

This linear set of coupled differential-difference equations can be solved using the discrete symmetry $u_i(t) = u_0(t+i/v)$ for the lattice points and thus $u_0(w) = \frac{f_0(w)}{1/d^2+2-2\cos(w/u)-w^2}$ where $f_0(w)$ is the Fourier transform of $f_0(t)$.Therefore the radiative resonances will occur according to the calculus of residues from the frequencies that cause the denominator of the above expression to vanish.

Therefore according to their explanation as time evolves the velocity of the kink drops and therefore the number of radiative frequencies causing the denominator to vanish changes. During the time of a certain number of resonant frequencies in the phonon band the energy loss is almost constant but as that number changes an abrupt decrease in energy loss occurs since the number of frequencies that emit radiation decreases. This is the way they define the so called quasi steady states in which the velocity of the kink is not changing very fast.These states can be identified as the average of the kink velocity oscillations observed in the kink velocity profile given in figure [5]. The nature of the oscillations will be explained later in the text but one can clearly see characteristic "knees" in figure [5] where the velocity profile of the kink is given for an initial velocity of 0.3. These knees also observed in [15] correspond to the quasi steady states.

Of course this approach seems to be reproducing quite well the qualitative picture of the problem and seems to be reproducing the quasi-steady state velocities to a high degree of accuracy however it seemed to us that the forcing of the kink towards the fluctuations should have a more physically clear origin than the mere introduction of a force-like term (2-nd derivative in time of the continuum solution).

Therefore our approach to this problem consisted of substituting in the equations of motion the ansatz:

$$y_i = q_i + k(i,t)$$

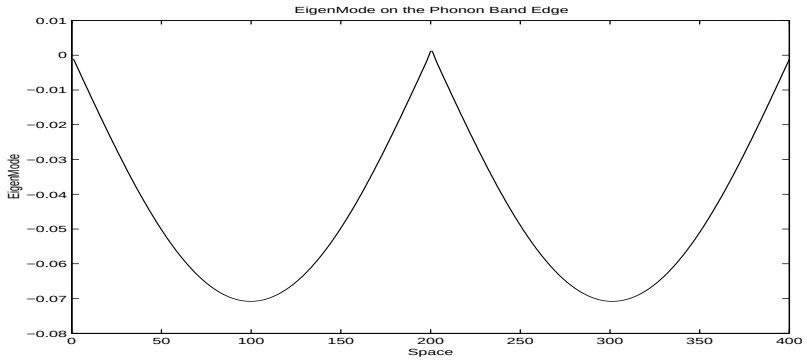


Figure 17: Delocalised Mode Close to the Lower Phnon Band Edge

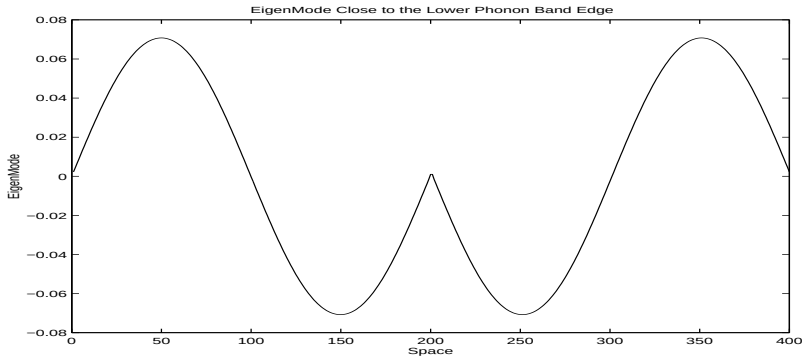


Figure 18: Plot of Another Delocalised Mode Close to the Bottom of the Phonon Spectrum

where $k$ is the discretized continuum kink and q are the fluctuations. Then considering to first order that $cosq \simeq 1$ one obtains the equation for $q_i$:

$$\ddot{q_i} = \Delta_2 q_i - \frac{1}{d^2}\sin(q_i)\cos k_i - \frac{\partial^2 k_i}{\partial x^2} + \Delta_2 k_i)$$

We then proceeded to solve this equation using the external driving $-\frac{\partial^2 k_i}{\partial x^2} + \Delta_2 k_i)$ as given in the equation above as well as by keeping the first term in the expansion $\Delta_2 k_i - \frac{\partial^2 k_i}{\partial x^2} = \sum_{j=2}^{\infty} \frac{2}{2j!}\frac{\partial^{2j} u_{ki}}{\partial x^{2j}}$ which is the 4rth derivative (i.e. $\frac{1}{12}\frac{\partial^4 u_{ki}}{\partial x^4}$) as a consistency check. The solution of this system was done coupled to the solution of the discrete F-K equations. In this way at each iteration we were updating the position of the kink using a linear interpolation scheme between the points right before and right after $\pi$ so that the position of the kink center was always at $\pi$: $X_{kink} = \frac{\pi - u(i,t)}{u(i+1,t)-u(i,t)} + i$. We selected a site which was during the simulation in the wake (and far away) from the kink and we show in figures [6]-[7] the power spectrum density of the resulting time series as arising from the simulation and from the model(d=1.15, $v_0 = 0.4$). One directly notices that despite the fact that the fluctuations are substantially stronger in the model (as it has also been observed elsewhere i.e. see [16]) however one still captures with this more physical model the main qualitative characteristics (i.e. the radiative frequencies) by this simple (and more natural than the one in [15]) model. Our simulations show also the same kind of agreement for the relevant frequencies in the power spectrum of the discrete Poynting flux which is defined as

$$S(i,t) = -\frac{u(i,t+dt) - u(i,t)}{dt}(u(i+1,t) - u(i,t))$$

A typical time-series of this quantity as arising from the above numerical experiment is given in figure [8] and its power spectrum given in the figure [9] again compares quite well with the characteristics that the corresponding power spectrum of the model of kink driven fluctuations exhibits.

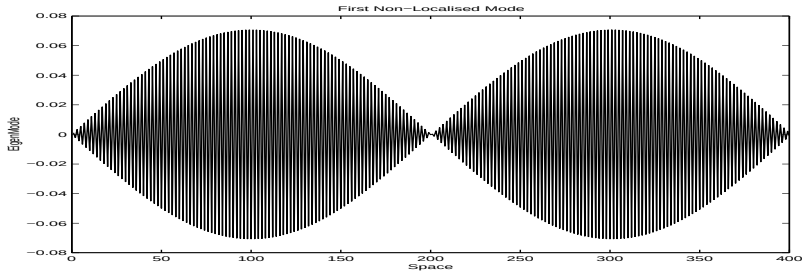


Figure 19: Delocalised Mode Close to the Top of the Phonon Band

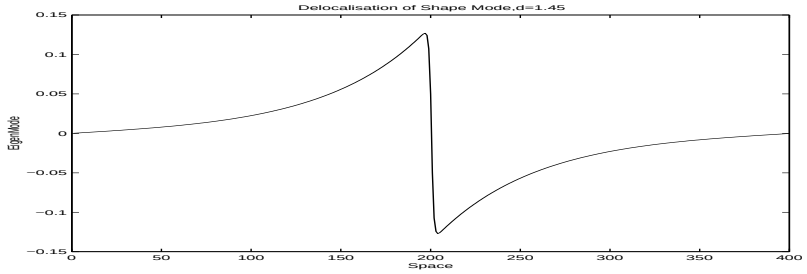


Figure 20: Delocalisation of the Shape Mode For Large d

At this point it would be interesting to introduce a collective variable theory that captures quite well the quantitative and qualitative features of the radiation emission process. This theory will be used for further comparisons with our predictions and with the numerical experiments both for the calculation of the Peierls-Nabarro barrier as well as for the problem of interacting kink structures.

### 2.4.1 Interlude II: BWS Collective Variable Theory

This theory was introduced in a number of a papers[16-23] by Boesch, Willis and Stancioff and their collaborators and will thus be subsequently referred to as BWS Theory. It essentially involves the discrete extension of a method introduced by Tomboulis [24] for the continuum problem which permits oneself to use 1 set of collective variables (X,P) for each kink involved in the problem under study and thus to follow the motion of the kinks as independent (collective) variables.

However the introduction of these 2 new variables generates a system of 2N+2 variables (where N is the number of lattice sites) whereas one has only 2N (first order) coupled differential equations.Therefore one needs 2 constraints in order to be able to solve the system.Suppose therefore that we introduce the ansatz $y_i = q_i + f_i(X)$ where f is the approximation to the kink continuum solution (or more generally something that describes the kink) whereas $q_i$ is a generic term incorporating the effects of fluctuations as well as the changes in shape of the original kink solution (the so-called dressing of the kink due to ,for example, the kink's internal modes which we will discuss later in the text).Their imposed equations of constraints are :

$$\sum f_i' q_i =< f_i' | q_i >= 0$$

$$\sum f_i' p_i =< f_i' | p_i >= 0$$

(from here on we will use both the sum and the Dirac notation and ' denotes differentiation w.r.t. X - the position of the kink). One motivation for the introduction of the first of the equations above (which first appeared in [25]) is that it is the outcome of the minimization of $\sum (y_i - q_i)^2$ therefore gives the "least squares fit" approximation to the shape of the kink.In [25] it was viewed as a way of minimizing the size of the domain walls.

In any case introducing these 2 extra new constraint equations $C_1 = 0$, $C_2 = 0$ where $C_1, C_2$ are the bracketed expressions in the equations used above one can solve the 2N+2 equations of the system and find in principle the

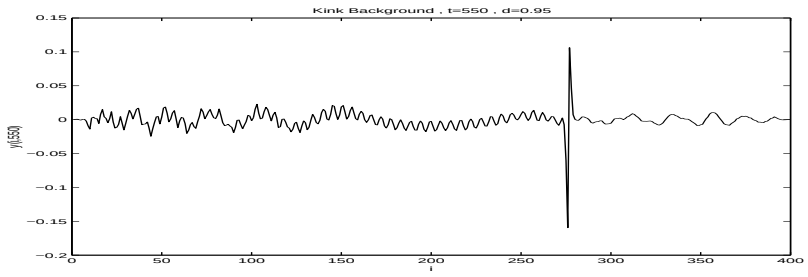


Figure 21: Background Profile Showing the Static Dressing (shape mode) and the Evanescent Wave Fluctuations

$q_i$'s as well as the position and the momentum of the collective variable describing the kink.However BWS found a way of a)formalizing and b)simplifying this procedure.

Their motivation in imposing these constraints was the fact that these constraints would nicely decouple the fluctuations and kink contributions in the Lagrangian and Hamiltonian description : Indeed considering $p_{y_i} = p_i + P$ (where the first term corresponds to the kinks and the second to the fluctuations one gets the Hamiltonian $H = \frac{P^2}{2M} + \frac{1}{2}\sum {p_i}^2 + \sum V(q_i + f_i)$ where the mass M of the kink is defined as $M =< f'|f' >$ However the existence of constraints according to the Dirac constraint theory [27] signifies that the Poisson brackets have to be modified to Dirac brackets in order for the new dynamical variables $q_i, p_i, X, P$ to satisfy the canonical commutation relations which the old dynamical variables $y_i, p_{y_i}$ satisfied (i.e. $[q_i, p_{y_j}] = \delta_{ij}, [q_i, q_j] = 0, [p_i, p_j] = 0$.Therefore the Hamiltonian formalism for a constrained system leads to the new canonical brackets $[q_i, p_j] = \delta_{ij} - [q_i, C_a]([C_a, C_b])^{-1}[C_b, p_j]$ (a,b take the values 1,2) . Using these brackets the reader can easily verify that the constraints are indeed verified at any moment in time :i.e. $\dot{C}_a = [C_a, H] = 0$. Therefore these are the appropriate brackets for the constrained system and now using Hamilton's equations $\dot{A} = [A, H]$ where A can be any of our 2N+2 dynamical variables one can obtain in a formal way the equations of motion for the system. This was the formal physically rigorous procedure.

However in a later paper the same authors developed a much faster and more elegant technique for deriving the same equations. Essentially 2N of the equations can be directly obtained by substituting the ansatz in the original F-K equation (which has to be true independently of constraints).Now by acting to the resulting equation with a symplectic projection operator $P_{nl} = \frac{|f'_n><f'_l|}{M}$ one obtains the exclusion of the solutions that do not satisfy the constraints. However then one has to operate again in the resulting equation with $< f'_n|$ in order to obtain a single equation for the collective coordinate $X$. This procedure , in the case of multiple collective variables (i.e. many kinks or anti-kinks), can be repeated for each collective variable yielding a second order equation for that collective variable. Furthermore, it can be simplified even more by using the properties of the projection operator (i.e. $< f'_n|P_{nl} =< f'_l|$ inducing the equations by a simple projection to the symplectic $< f'|$ space which will signify direct realization of the constraint.

In the case of the single kink + radiation effects (or more generally fluctuation effects since q also includes the shape modifications of the kink due to discreteness) applying this methodology one obtains the equations :

$$f'\ddot{X} + \dot{X}^2 f'' + \ddot{q} = \Delta_2(f+q) - \frac{\partial V}{\partial q}(f+q)$$

$$M\ddot{X} = - < f'_i|\ddot{q}_i > + < f'_i|\Delta_2(f+q)_i > + \dot{X}^2 < f'_i|f''_i > - < f'_i|\frac{\partial V}{\partial q}(f+q)_i >$$

For the practical purpose of solving numerically the coupled equations one more step needs to be taken in order to render the prescription numerically tractable. That involves the differentiation(twice)of the constraint 1 which yields $< f'_i|\ddot{q}_i >= -\ddot{X} < f''_i|q_i > -\dot{X}^2 < f'''_i|q_i > -2\dot{X} < f''_i|\dot{q}_i >$. Substituting this equation to the second of the equations above one can solve it for $\ddot{X}$ and then back-substitute to solve equation (1).

We chose to introduce this theory at this particular point not only because of its successful predictions in the coupled kink- fluctuations problem but also for pedagogical reasons since this seems to us to be its most natural application domain.

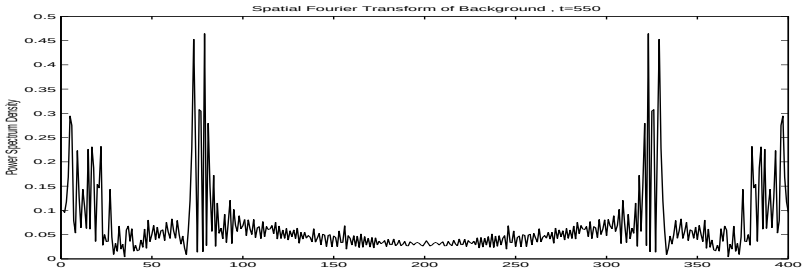


Figure 22: Spatial Fourier Transform Power Spectrum Corresponding to fig. [24]

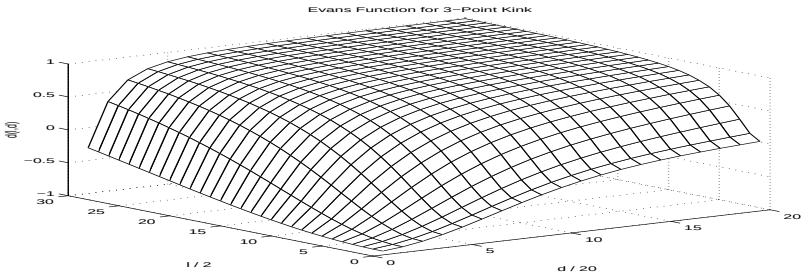


Figure 23: 3 Dimensional Plot of the Real Evans Function $D(d, \lambda)$ for the 3 Point Kink

In fact using this theory BWS were able to present in their papers the most satisfactory ,to date, picture of the radiation problem.

In order to understand their explanation we have to introduce some notions of scattering theory which we will present in the next subsection

### 2.4.2 Interlude III: Scattering Theory

The phonon spectrum of the linearized continuum Sine-Gordon equation is well known to be $w^2 = \frac{1}{d^2} + k^2$.In the discrete case as can be seen by either substituting the same plane wave solution $(\exp(i(kx - wt)))$ or by rescaling d this becomes the equation for the discrete spectrum $w^2 = \frac{1}{d^2} + 2 - 2\cos(k)$ and we see that because of the existence of a minimum wavelength of wave that can propagate in the lattice ($\lambda = a$ where a is the lattice spacing ) there is a maximum permitted wavenumber and thus discreteness restrains the continuous spectrum to the frequency range $(\frac{1}{d^2}, 4 + \frac{1}{d^2})$. Apart from these continuum states there are also bound states that can be found using the ansatz:$y = y_k + \psi$ with $\psi(x,t) = \psi(x)\exp(-iwt)$. The corresponding Schrodinger-like bound state problem then is described by the equation:

$$f_{xx} + \frac{1}{d^2}V''(y_k)f = w^2 f$$

and has always as one solution the so-called GoldStone mode which corresponds to the eigenvalue $w = 0$ with corresponding eigenvector $f = y_x$ (i.e. see fig. [16]). which is ,in the Sine-Gordon case, $\propto \frac{1}{2d} sech\frac{x}{d}$ whereas for $\phi^4$ it is $\propto sech^2(\frac{x}{2d})$. In the sine-Gordon equation this mode is the only bound state solution in the continuum case. However this is not generically true since for example the $\phi^4$ model has another internal oscillation of harmonically varying shape change of the kink which has eignevalue $w_2 = \frac{\sqrt{3}}{2d}$ and corresponding eigenmode $f = \frac{3}{4d} sech\frac{x}{2d}\tanh\frac{x}{2d}$. These internal modes lie of course between 0 and 1/d (the lowest edge of the phonon band).Let us also mention in passing that these 2 particular potentials are reflection-less which means that the particles in passing through the potential will not be reflected (i.e. develop an eigenfunction component at later times which is $\propto \exp(-i(kx \pm \delta(k)))$ but rather will only suffer a phase-shift in their original wavefunction. This property is non-generic in non-linear Klein-Gordon potential (i.e. the DSG or the double quadratic potential don't share this property).

Thus having closed this interlude of continuum soliton problems, let us now explain by means of the modifications

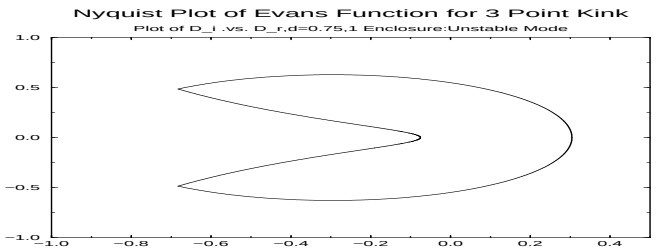


Figure 24: Nyquist Plot of the Evans Function $D(i\lambda)$ Showing the Instability of the 3 Point Kink (d=0.75)

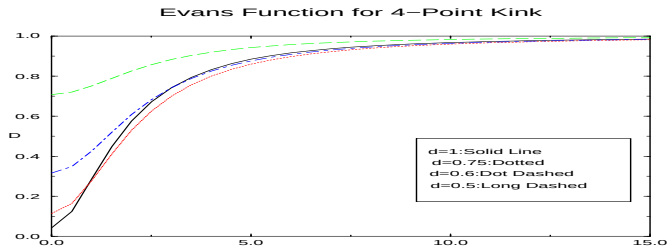


Figure 25: Plot of the Real Evans Function $D(\lambda)$ for Various Values of the Discreteness Parameter d for the 4 Point Kink

of this picture the kink-radiation problem.

In the discrete case the Goldstone mode is still present as the bound state of the kink but no longer has zero frequency (rather its squared frequency gets shifted from zero becoming positive or negative depending on the stability of the kink (i.e. on whether its center lies on or between lattice points). In the former case (center on lattice points) a negative result yields one growing and one decaying mode (the time symmetry imposes the existence of two symmetric modes).On the other hand the positive result in the latter case verifies its stability. Our stability analysis given below both by eigenvalue solutions as well as by use of Evans functions will clarify that point later in the text.

Also, there exists a characteristic frequency associated with the soliton propagation over the PN wells which is $W = 2\pi\dot{X}$ where $\dot{X}$ is the velocity of the kink. Depending on the initial kink velocity for cases of sufficient discreteness some of the harmonics of this characteristic frequency will be lying inside the phonon band $(\frac{1}{d^2}, 4+\frac{1}{d^2})$.It is precisely the resonance of these frequencies with the phonon frequencies which will cause the radiation effects and it is these same frequencies that caused the poles to occur in the Peyrard and Kruskal model. As time progresses the velocity of the kink decreases and therefore so does its characteristic frequency. Hence, its harmonics will pass from the lower band edge of the spectrum being unable to radiate any more. Hence one can retrieve the quasi steady state velocities as $\dot{X} = \frac{1}{2d\pi n}$ getting very good agreement with the numerical experiments of [15]. As we approach these quasi steady states the radiative effects can be seen to significantly decrease (a spatial velocity profile close to a quasi steady state for the case of a kink starting with $v = 0.8$ in the $d = 1.0$ case is shown in the figures [10]-further away for the Q-S.S. one observes stronger oscillations). This gives a satisfactory explanation of the characteristic knees observed in the velocity time evolution profile as well as in the energy loss .vs. velocity plot of [15]).Of course one could argue that at the same time higher harmonics will be penetrating the spectrum yielding new resonances and producing radiation.However one should keep in mind that discreteness signifies that the existent wavenumbers are of the form $2\pi/(na)$ and thus they are piled up close to the lower band of frequencies where there is a high density of states N rather than on the top of the band. Therefore these effects are less easily observable than the previous ones since they occur in the upper sparsely populated edge of the phonon band.

In fact the resonance picture permits one to understand the behavior of the kink even at quite late stages. As the process of radiation continues the kink loses gradually more and more of its original energy and finally gets trapped in the Peierls- Nabarro barrier. In that case there as we saw in the previous section the kink while trapped performs oscillations between the unstable position of the potential energy maximum and the stable one of the corresponding

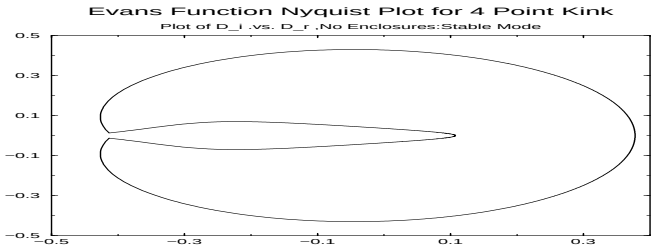


Figure 26: Nyquist Plot of the Evans Function for the 4 Point Kink in the case of d=0.75

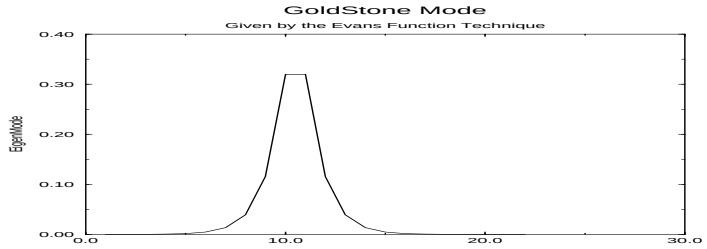


Figure 27: The GoldStone Mode as Given by Newton Iteration Root Finding of the Evans Function

minimum (0, 1/2 (mod 1)respectively). In that motion however there is another characteristic frequency (the Peierls-Nabarro frequency defined by the curvature (the value of $V''$) at the bottom of the potential well). Initially some high order harmonics of this frequency will exist in the phonon band creating resonance effects once again inducing radiation from the kink.Therefore the energy of the kink decreases further signifying a corresponding frequency increase which will permit further harmonics to resonate with the phonon band frequencies and therefore the opposite effect will be gradually occuring i.e. radiative bursts (which BWS first noticed and reproduced by means of their collective variable theory) from resonant harmonics crossing the high density of states lower band edge of the phonon spectrum (again the gradual cross-out of the higher harmonics off the higher band edge of the spectrum will not be clearly discernible).This energy loss be it gradual or abrupt will finally result in the complete halt of the kink motion at its equilibrium position. These phenomena , which are verified also by our numerical observations demonstrate the radical change of the picture one has of continuous solitons as one goes to discrete lattices.

The BWS theory was particularly successful in revealing these phenomena. In fact it was able to predict another rather interesting characteristically discrete bursting phenomenon in which the kink as driven by fluctuations to bursts out of a certain half lattice point's Peierls-Nabarro barrier (obtaining energy to surpass the barrier by means of the radiative driving) and oscillates in a different barrier rather than in the one in which it was originally trapped.

This predictive success of the BWS theory demonstrated its agility in following the motion of the single collective variable as well as in predicting the phenomena occurring in the MD simulation. However we should note at this point that in a sense we should be expecting such a success since in principle all that one is doing in applying the BWS theory is effectively a change of variables which permits one to follow the motion of the kink(adding 2 equations to the ones one has to solve). Now given these tools (i.e. BWS theory) let us go back and revisit the subject of the Peierls-Nabarro barrier and compare the various theoretical predictions.

## 2.5 Peierls-Nabarro Barrier

In the paper where they introduced the Hamiltonian constraint theory formalism BWS derived the Peierls-Nabarro barrier for the case of the single kink in a discrete lattice neglecting fluctuations. The differential equation arising from their formalism in order to describe the kink motion is:

$$\ddot{X} + \frac{\dot{X}^2}{2}\frac{dlnM}{dX} = -(1/M)\frac{\partial V(q_l + f_l)}{\partial X}$$

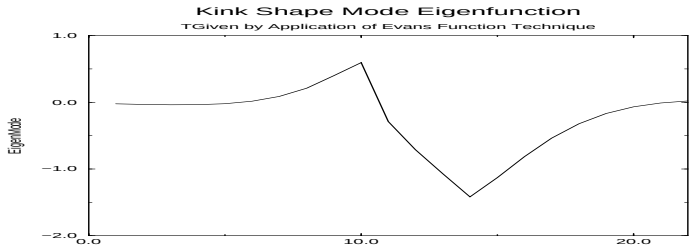


Figure 28: The Internal Shape Mode as Identified by the Above Method

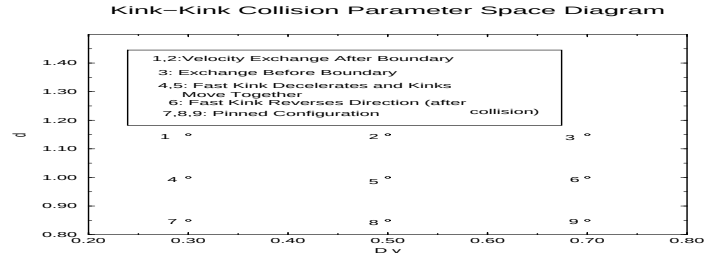


Figure 29: Kink-Kink Collision Parameter Space Phase Diagram

Therefore in their first approximation they neglected the small variation in the kink mass $M =< f'|f' >$ with respect to X and also neglected fluctuations to get the equation:

$$\ddot{X} = (1/M) < f'|(f_{i+1} + f_{i-1} - 2f_i - \frac{1}{d^2}\sin f_i >$$

They, then, went on to analyse this "bare" (i.e. not dressed by fluctuations of the shape of the kink ) calculation to an approximate one in which they use only the first order correction term of the second difference expression as a sum of derivatives (given above). In that case the equation reads : $\ddot{X} = -(1/M)\frac{\partial U}{\partial X}$ where $\frac{\partial U}{\partial X} = -\frac{1}{12}\sum_i < f'|f'''' >= \sum_i B_i \sin 2\pi i X$ with $B_i = \frac{\pi^3 i^2}{3\sinh i\pi^2 d}(2i^2\pi^2 + 1/d^2)$. However since the potential will have the cosinusoidal form of $U = U_0 + \frac{E_{p-n}}{2}\cos 2\pi X$ where $E_{p-n}$ is the Peierls-Nabarro barrier due to discreteness $\Rightarrow E_{p-n} \simeq \frac{\pi^2}{3\sinh \pi^2 d}(2\pi^2 + 1/d^2)$. This expression gives the right growth rate for the potential barrier. The approximation of keeping only the first term in the cosine expansion is a quite successful one since the next term is around 3 orders of magnitude less (the approximation is better for larger d but in principle is appropriate for all the range of d's of interest (0.4-1.2)). However this calculation yields predictions that are quite smaller than the actual barrier as calculated from the simulation as shown in figure [11].Of course it becomes a better approximation as one approaches the continuum limit however it fails quite drastically as our calculations indicate in the discrete case. In fact as the same authors indicate this first order approximation is better than the full bare calculation (the one not neglecting the higher order terms). Therefore clearly something should be incorrect in this scheme.

Our variational calculation yields the same equation as their initial equation for our variational parameter X (differentiating the energy integral w.r.t. time):

$$M\ddot{X} + \frac{1}{2}\frac{dM}{dX}\dot{X}^2 = -\frac{\partial V}{\partial X}$$

However notice that if one supposes the mass to be (first order approximation) independent of X , then the term $\frac{1}{d^2}(1 - \cos(f))$ using the ansatz $f = 4\arctan(\exp(k(i - X)))$ is equal (using trigonometric identities) to a term $\propto \frac{1}{\cosh(k(i-X))^2}$ which in turn is $\propto M$. Hence if one ignores the effects of mass variation in the $\dot{X}^2$ term self-consistency imposes a similar approach to the second term of the potential. However doing that one obtains a relatively good (again) approximation to a cosinusoidal potential well. This was shown in the figure [3] , comparing the full potential well as obtained by using $U = \sum_i(\arctan(\exp(k(i + 1 - X))) - \arctan(\exp(k(i - X))))^2$ for a

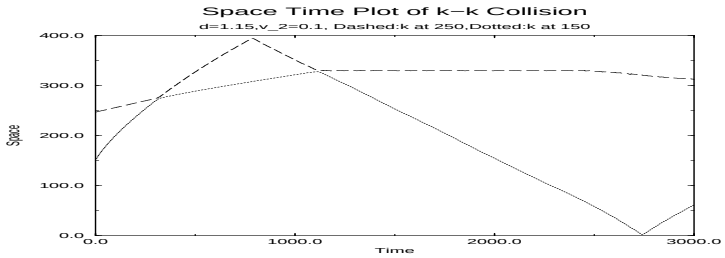


Figure 30: Space-Time Plot of Kink Positions for the Collision with d=1.15, $v_2 = 0.1$

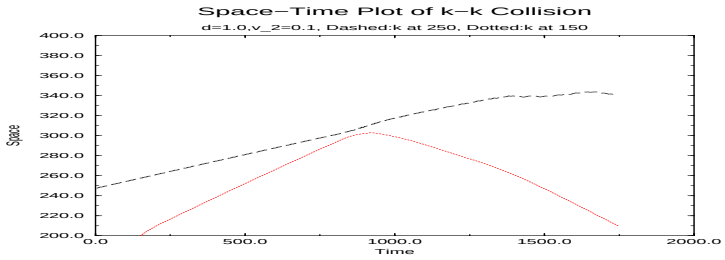


Figure 31: Same as Above for the Collision with $d = 1.0, v_2 = 0.1$

400 point lattice and comparing it with the first order cosine term (this approximation and the effective potential treatment given before yield approximately the same potential barrier due to the consistency of the approximation). The first order cosine approximation for a function $q(x) = \sum_i f(i-x)$ is given by $q(x) = \frac{A_0}{2} + A_1 \cos(2\pi X)$ whereas in general:

$$q(x) = \frac{A_0}{2} + \sum\nolimits_{n=1}^{\infty} A_n \cos(2\pi n X) + \sum\nolimits_{n=1}^{\infty} B_n \sin(2\pi n X)$$

with $A_n = 2\int_{-\infty}^{\infty} f(z)\cos(2n\pi z)$ and $B_n = -2\int_{-\infty}^{\infty} f(z)\sin(2n\pi z)$ and with $z = i - X + 1$ (for a more detailed presentation of Fourier analysis of sum functions on a lattice see [17]).

The depth of the potential that was self consistently (i.e. neglecting the mass dependence on X in all the cases in which it arises) calculated through our variational technique is compared to the actual experimental Peierls-Nabarro barrier as well as with the BWS calculation in figure [11].One can clearly see that as discreteness (and therefore static dressing , shape mode as well as radiative driving effects) become important both BWS and the variational approach leave a lot to be desired since this is all that one can capture out of the full problem with just one collective variable. However notice that the self consistent variational approach is consistently closer to the actual barrier than the BWS calculation. The same is true in comparison to the Ishimori and Munakata ([26]) estimate of the Peierls-Nabarro barrier (in our units) $E_{p-n} \simeq 29.728 d \exp(-\pi^2 d)$ which is not shown in our plot but is shown in Fig.1 of ref. [20] to give even worse results than the bare approximation of BWS -i.e. notice that the barrier goes to 0 for $d \to 0$-.The Ishimori and Munakata calculation essentially uses the Keener-McLauglin perturbation theory [27] considering discreteness as a perturbation to the bare continuum ground state. Thus, one knows that for sufficiently large discreteness (small values of d) this will not be a realistic treatment of the system due to the dramatic intrinsically discrete effects that appear. Therefore we conclude that our variational approach is consistently the best one-parameter approximation to (at least) the qualitative behavior of the Peierls-Nabarro potential barrier.

However in one of the subsequent papers BWS found a way to calculate the Peierls-Nabarro barrier to a very good approximation. Their method involved the exact calculation from simulations of the exact ground state of the system (arising from the relaxation of the kink in the P-N well by gradual drainage of its energy).Given this exact ground state (which bears the inherent characteristics of discreteness , rather than being a discretization of the continuum solution) one can expand the solution as:

$$\hat{f}_i(1/2) = f_i(1/2) + \int_{1/2}^{1-X} \psi_i(X'(t))dX'$$

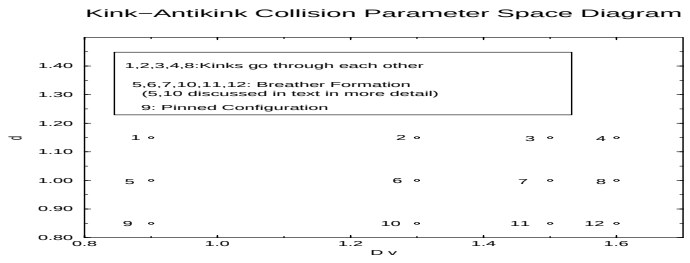


Figure 32: Kink-AntiKink Parameter Space Phase Diagram

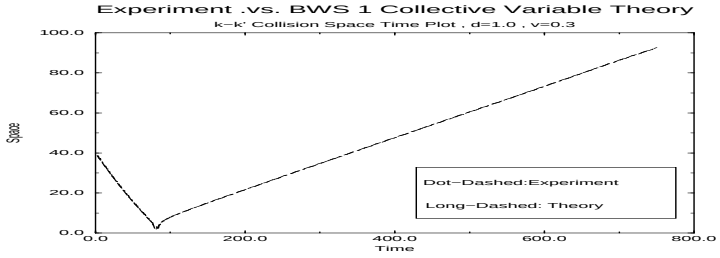


Figure 33: Space-Time Plot of the Relative Distance of the Kink and the Antikink for a Collision in Which they go through each other

Substitution of this ansatz in the equation for the kink (as derived in the BWS theory) and subsequent linearization around the equilibrium point $X = 1/2$ yields the equation for the kink position:

$$\psi_i(1/2)\ddot{X} = -[\hat{L}\psi_i(1/2)](X - 1/2)$$

where the operator $\hat{L}$ is defined as $\hat{L} = {w_0}^2 \cos(f_i(1/2)) - \Delta_2$. Therefore solving the eigenvalue equation $\hat{L}\psi_i(1/2) = {w_b}^2\psi_i(1/2)$ one obtains the frequency of the kink oscillations in the Peierls-Nabarro well. This method predicts very accurately the values of the depth of the well as well as of the frequency of oscillation (related in essence with the curvature of the well at its bottom) however one should bear in mind that practically it involves the exact M-D assisted determination of the ground state configuration.Also it no longer hinges on the single- collective variable 1-parameter determination of the barrier but it incorporates the effects of discreteness in statically dressing the kink i.e. modifying its shape as it propagates through the lattice.

In any case it provides a strong quantitative understanding of the fact that one should not use continuum ansatze in intrinsically discrete situations nor should one treat discreteness as a perturbation since the principal exhibited characteristics are by nature different than their continuum counterparts.

A last point worth mentioning in passing about the Peierls-Nabarro barrier is the fact that it has been suggested in the bibliography that the existence or non-existence of it in a discrete system might be a valid diagnostic concerning the integrability of the discrete model. The interested reader can refer to [28] for more details on this conjecture.

## 2.6 Kink Motion

In terms of phase space the kink constitutes an heteroclinic connection between the two unstable equilibria (0 and $2\pi$ mod $2\pi$ ) of the Sine-Gordon potential. This is clearly demonstrated in the figure [12] in which for different times the positions and velocities of the 400 lattice sites of the simulation are plotted. In this way instead of plotting the motion of a single point over infinite time to trace the heteroclinic connection one can do so by plotting the velocities .vs. the positions of the 400 lattice points of the kink. Most of the points will pile up at 0 or $2\pi$ but the points constituting the spine of the kink will trace the kink heteroclinic connection in the phase space.

In order to understand more about this phase space picture it would be useful to understand in more detail the

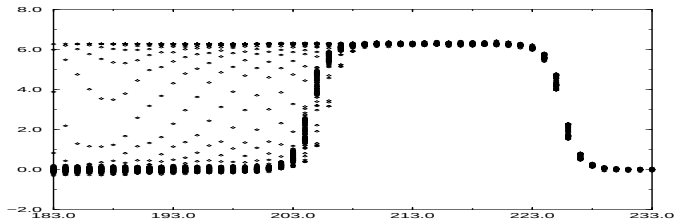


Figure 34: Static Configuration of a Pinned $k - \bar{k}$ Pair

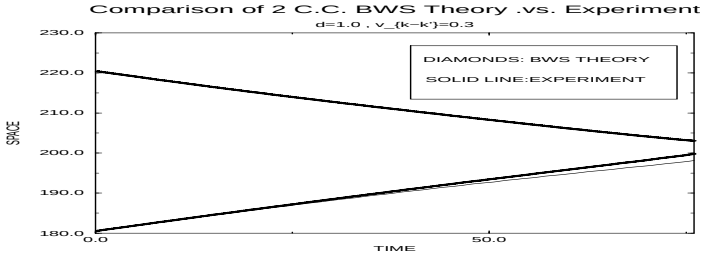


Figure 35: Comparison of 2 Collective Variables BWS Theory With Experiment in a Space Time Plot of $k - \bar{k}$ Pair Positions

motion of the kink as driven by the fluctuations. Let us remind the reader that at no point so far did we consider the fluctuation effects in the form of the evanescent background phonon radiation.The driving of the kink as a result of these fluctuations has to be taken into account in order to understand more about the kink motion.

In one of the early works on the subject ([15]) Peyrard and Kruskal presented numerical simulations in which the velocity of the kink seems to be strongly oscillating (figs. 3,4 in ref. [15]).In another early work in the subject Combs and Yip introduced the notion of the constraint $< f'|q >= 0$. Differentiating the equation of the constraint twice one can get an equation for the motion of the kink (A 14 of ref. [25]):

$$M\ddot{X} + [-2k^2 < f''|\dot{\psi} >]\dot{X} + (k^3 < f'''|\psi > -k^3 < f'|f'' >)\dot{X}^2$$

This equation was claimed by the authors of [25] to be a generalised Langevin equation that the motion of the kink follows. In fact in a subsequent paper ([31]) the same authors presented molecular dynamics evidence of velocity autocorrelation plots as well as of mean square displacement over time which illustrate their original claims about diffusive (Brownian) motion of the kink when driven by the fluctuations in the lattice. We present in figures [13],[14] graphs of the velocity autocorrelation function $\psi(t) =< v(t)v(0) >$ as well as of the mean square displacement over time as arising from our numerical simulations.As is well known in the theory of diffusion the slope of the mean square displacement function gives the self- diffusion coefficient according to the formula:

$$D_k = \lim_{t\to\infty} \frac{W(t)}{2t}$$

where $W(t) =< (X(t) - X(0))^2 >$.On the other hand the velocity autocorrelation is also related to the self diffusion coefficient according to the formula: $D_k = \int_0^\infty dt < v(t)v(0) >$. As our plots demonstrate the assumption of diffusive motion seems quite plausible since at long times the slope of the mean square displacement seems to be tending to a constant yielding the diffusion coefficient (also for short times it seems to be linearly growing in time as predicted by the theory of Brownian diffusion). Furthermore our velocity autocorrelation results seem to be comparing quite well with the results obtained in [31] for. However one important point that should be kept in mind is that this picture of diffusive kink motion as driven by fluctuations should be superimposed to the picture of the kink velocity being modified by bursts of radiation when because of the resonances of the velocity harmonics with the phonon spectrum.Therefore the kink seems to be performing Brownian motion with gradually decreasing velocity because of small radiative losses (being on the average close to what Peyrard and Kruskal call a quasi-steady state).Therefore

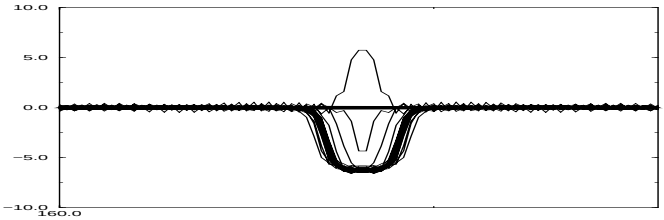


Figure 36: Pinned Implosion due to Small Initial Distance of $k - \bar{k}$ Pair for d=0.785 and k at 195, $\bar{k}$ at 205

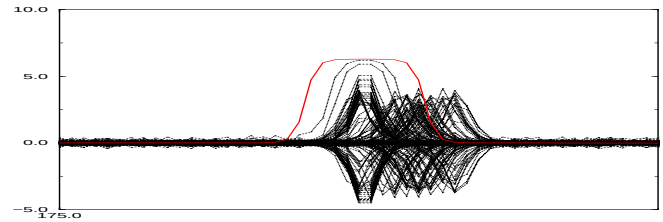


Figure 37: Propagating Breather Formation for Same I.C. as Above at Lower d(=0.7)

the picture given before about radiation rates and resonances of quasi steady states with the phonon spectrum holds true on average whereas the detailed motion of the kink in these quasi steady states consists of diffusive driving of the kink from the existing fluctuations on the lattice.In the first paper about the Hamiltonian version of the BWS theory ,Willis, Stancioff and Batanouny proved that self-consistent application of the Dirac constraint theory requires a refined version of the C-Y equation:

$$\ddot{X} + \frac{\dot{X}^2}{2}\frac{dlnM}{dX} = -(1/M)\frac{\partial V(q_l + f_l)}{\partial X}$$

which does not seem to substantiate the claim of diffusive kink motion. However all the above numerical evidence is strongly in favor of this suggestion and in fact one can prove theoretically that the kink is evolving in time through a non-linear generalized Langevin equation.This was done by Willis and Batanouny ([32]) by means of evaluation of the radiative damping of the kink and using the fluctuation dissipation theorem to obtain the appropriate fluctuation force.However we will not reproduce the details of this calculation here. Let us also note that claims of Brownian motion of a kinks have appeared also in the context of 1d double well field theories (i.e. see [33]).

## 2.7 Kink's Internal Modes

In a very interesting recent paper Braun et al. ([34]) revealed another very interesting manifestation of discreteness which is not shared by the continuum counterpart of the lattice solitons.

In our scattering theory interlude we saw that Schrodinger equation type of scattering theory for the case of perturbative excitations around the kink solution revealed the existence of a single bound state mode belonging to the kink and corresponding in the continuum case to the symmetry of translational invariance thus yielding a zero eignfrequency.As was pointed out one of the effects of discreteness is to move that eigenfrequency away from zero (since translation invariance is lost). However in a sense this result is a quite plausible extension of the continuum picture in the discrete version. What was surprising and new in [34] was the appearance in the case of the discrete problem of a new fundamentally discrete shape mode of the kink that no longer corresponds to the GoldStone mode of $sech(k(i - X))$ but in fact is an odd parity mode (see figures [15]-[[19] for comparison of the corresponding

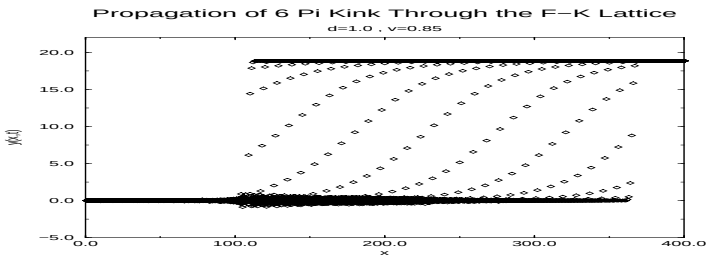


Figure 38: Fast Propagation of a 6 $\pi$ Kink Through the F-K Lattice

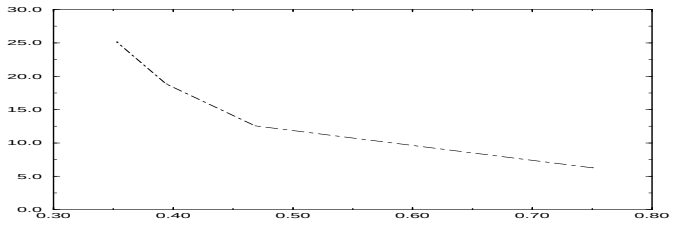


Figure 39: Pinning-Depinning Phase Transition for High Amplitude Kink Motion

eigenfunctions).This study ([34]) was mainly focused on the properties of the Peyrard-Ramoissenet potential :

$$V(u) = \frac{(1-r^2)(1-\cos(u)}{1+r^2+2r\cos(u)}$$

This potential (hereafter referred to as PR ) was introduced by Peyrard and Ramoissenet in [35] in order to study the variations of the discrete lattice soliton solutions (kinks or breathers) as a function of the variation of the potential shape. The subcase of r=0 corresponds to the Sine-Gordon potential whereas for small values of r the potential reduces to the double Sine-Gordon potential $V(u) \propto -\cos(u) + r\cos(2u)$.

Thus,in order to study the frequencies appearing in the spectrum of the discrete static kink Kivshar et al. determined numerically the static configuration corresponding to minimum energy of the kink for a certain choice of boundary conditions and using the numerical evaluation of the lattice point positions they solved the eigenvalue problem (now for a matrix rather than for a continuum operator arising from the substitution of the ansatz $u_i = {u_i}^{eq} + v_i \exp(iwt)$. The resulting matrix eigenvalue equation will then read $Av = w^2 v$ where A is a tridiagonal matrix of entries $A(i,i) = 2 + \frac{1}{d^2}V''({u_i}^{eq})$, $A(i,i+1) = -1$, $A(i,i-1) = -1$. By solving the eigenvalue problem we verified their results that for certain values of the discreteness parameter d there exists a range of parameters of the potential r (the range is larger for smaller values of d - i.e. see figure 1 of [34]) for which one of the kink characteristic eigenfrequencies separates from the edges of the phonon spectrum and makes an excursion in the spectral imaginary axis outside the phonon band. For small values of r the excursion occurs at the lower edge of the continuum spectrum and signifies a low frequency shape mode (shown in figure [19] in the case of r=0 -discrete SG- for d=0.7) whereas for large r it occurs from the top band of the phonon spectrum creating a high frequency mode above the top band of the phonon spectrum (i.e. shown in figure 4 of [34]). This localised low frequency shape mode which is a characteristic of discreteness, starts out as a quite localised mode around d=0.5. As d increases one approaches the continuum and the excursion from the phonon band gets smaller. Thus for example in the case of d=0.7 (which can be characterized as typical of this behavior since the system is sufficiently discrete) one finds that the square frequency of the GoldStone mode is 0.1958 whereas the kink shape mode has $w^2 = 1.7898$ which is clearly separated from the bottom edge of the phonon band for which $w^2 = 2.04$. The eigemodes close to the band edge of the phonon continuum and typical delocalised continuum eigenmodes are shown in figures [17]-[19].

As one increases d reaching i.e. d=1.2 one finds that gradually the shape mode approaches the continuum spectrum (i.e for d=1.2 $w^2_{shape} = 0.6928$ whereas $w^2_{phonon} = 0.6947$ ) and thus the shape mode gradually gets

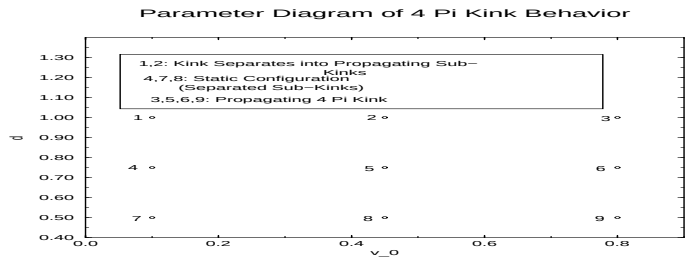


Figure 40: Parameter Space for the Behavior of the 4 $\pi$ Kink

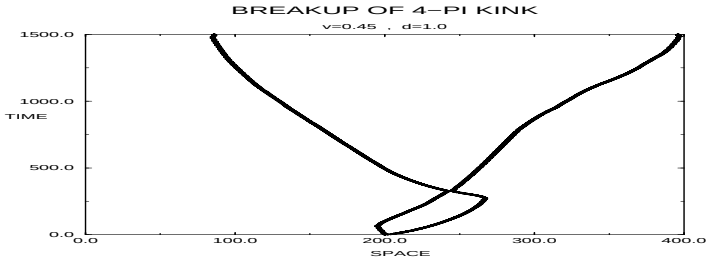


Figure 41: Breakup of 4 $\pi$ Kink Due to Low Initial Velocity (v=0.1)

delocalised (as seen in figure[20]).The same is true for much higher d (i.e. even for d=1.65 one can trace this mode now completely delocalised but still sitting slightly away from the phonon band).

Another nice way of tracing out this kink shape oscillation mode is by taking a snapshot of the spatial profile of the lattice propagation of a kink in the discrete SG case and subtracting out the continuum soliton. Then one is left with a radiation field plus the dressing of the kink (the shape mode) as is shown in figure [21] (also shown in figure [22] is the Fourier transform in wavenumber space of the spatial profile. There, one sees resonances that can be related tothe ones caused by the kink frequency -and its harmonics- in the phonon band, by means of the dispersion relation). This is in fact the physical basis of the BWS theory ansatz solution. And, that is why one of the early successes of this theory was its ability to predict this internal shape dressing of the kink. This was done in the second BWS paper where the properties of the static kink were investigated by using a dressing ansatz as mentioned above and by implementing a Lagrange multiplier approach that held the kink center fixed even at a non-equilibrium position. Their findings demonstrated the existence of the shape mode of the kink (see figure 1 of ref. [16]) and in fact revealed the existence of oscillations of the shape mode for sufficiently low values of the discreteness parameter d.

Recently Kivshar et al. ([42]) proposed a method for explaining the appearance of the internal shape mode of solitonic excitations. Their method was based on the consideration of the term from which the non-integrability of the system arises (their technique appears to be generic for non-linear non-integrable models) as a perturbation of the corresponding integrable equation. Their presentation involves the kink of the double sine- Gordon that is well known to have internal shape modes. In that case given the continuum nature of the equation it is not surprising that the method works. However it seems quite striking that the method seems to go through in terms of accounting discreteness effects in the case of the shape mode (i.e. in the discrete $\phi^4$ model), especially since treatments of discreteness as a perturbation had been proved to be inadequate (i.e. the Ishimori and Munakata treatment of the Peierls-Nabarro barrier) in the past.

Supposing discreteness as perturbation one can write the discrete SG equation as:

$$u_{tt} = u_{xx} + \sin(u) + \epsilon g(u) = 0$$

where i.e. we know that the g(u) in the case of interest (F-K model) will be $\sum_j \frac{2h^{2j}}{2j!} \frac{\partial^{2j} u}{\partial x^{2j}}$. Then a perturbative

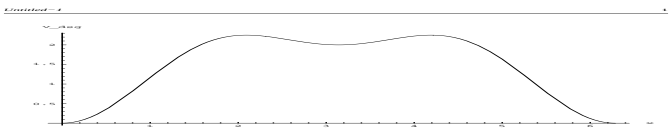

Figure 42: Double Sine Gordon Potential

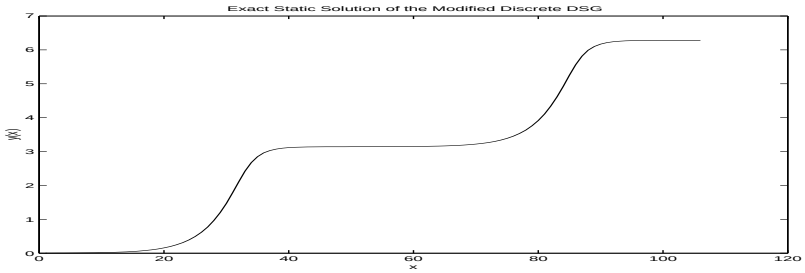


Figure 43: Exact Static Kink Solution of the Modified Discrete Double Sine Gordon Equation

expansion around the kink solution of the form $u = u_0 + \epsilon u_1$ with $u_0 = 4\arctan(\exp(x))$ one finds that

$$u_1 = \frac{1}{\cosh(x)} \int_0^x dx' \cosh(x')^2 \int_0^{x'} \frac{g(u_0)}{\cosh(x'')} dx''$$

Then the oscillatory excitations around the kink solution u can be written as $q(x,t) = w(x)\exp(iwt) + C.C.$ where w is the eigenvalue which arises from the solution of the eigenvalue problem after substitution of the ansatz $f = u + q$ in the original equation. The eigenfunctions of the unperturbed problem are known from the quantum mechanical scattering theory introduced before in the case of the SG equation to be $W(x) = \exp(ikx)(k + i\tanh(x))/(k + i)$. One directly notices that there is only a phase shift from the original incoming wavepacket which signifies that it does not get reflected from the SG potential (which is a requirement for the theory to work). It is intuitively clear that discreteness will cause the deformation of the eigenfunctions as well as the shift of the eigenvalues. But what one can see by expanding w in the full set of discrete and continuum states basis set of the integrable Sine-Gordon (W(x) plus the discrete GoldStone mode $W_{-1}$) is that if the perturbation has the right sign it will cause the birth of an additional discrete eigenvalue that will bifurcate from the continuum spectrum. It is possible to calculate the coefficients $a$ of the expansion $w(x) = a_{-1}W_{-1} + \int_{-\infty}^{\infty} a(k)W(x,k)dk$.Hence by evaluating the singular contributions to the integrals yielding the $a$'s the authors of [42] obtained an equation for the excursion parameter k ( the excursion is $\epsilon^2 k^2$ ) of this new eigenvalue from the bottom edge of the phonon spectrum. Their expression was:

$$|k| = \frac{sgn(\epsilon)}{2} \int_{-\infty}^{\infty} tanh(x)[p(x) + g'(0)]tanh(x)dx$$

with $p(x) = u_0 \sin(u_1) - g'(u_0)$. Applying this theory to the discrete $\phi^4$ yields a deviation from the continuum (considering the lowest order -i.e 4rth order- perturbation) of magnitude $\frac{4h^2}{15}$ which appears to be in good agreement with the simulations. However, there appear to be a number of problems with this explanation. First of all the authors of [42] when referring to the $\phi^4$ model they quote the equation for the first order perturbation as $u_{tt} = u_{xx} + 2u - 2u^3 - \epsilon u_{xxxx}$ with $\epsilon$ being in their paper $h^2/12$. However the equation for the analysis of the second difference as a sum of even order derivatives reads (see i.e. [25]): $\Delta_2 u = \sum_j \frac{2h^{2j}}{2j!} \frac{\partial^{2j} u}{\partial x^{2j}}$. This in turn signifies that the perturbation should have the opposite sign ! Furthermore we attempted to use their prescription in the case of the Discrete Sine Gordon equation (which is the most natural examination point for the validation or invalidation of this theory's ability to predict the birth of internal shape modes. In that case first of all the term $g'(0)$ in the

expression for the shift of the bottom edge of the phonon band will be absent since the bottom of the band edge remains unshifted (for k=0 $k^2$ and its discrete modification $2-2\cos(k)$ yield the same result (=0)). Furthermore the operator $g'(u_0)$ now becomes (following the steps of the linearization in deriving the equation that w has to satisfy) merely the 4rth order operator operating (for the calculation of the correction $|k|$) on $\tanh(x)$. If one considers the first order correction, one can perform the integration and find $u_1$ to be :

$$u_1 = (-\frac{1}{4} + \frac{23 - \exp(-2x) + \exp(2x) + \exp(4x) + 8(1 + \exp(2x)x)}{48(1 + \exp(2x))})$$

In that case however the integral involved in the calculation of $|k|$ seems to be diverging in our preliminary calculations. Furthermore the 4rth order derivative's contribution appears to have the wrong sign (as can be seen by plotting the function $f\tanh(x)$). If one considers higher order corrections they will have the right sign (justifying the "obscure" comment made in [42] about the Discrete SG problem ) but they will still yield exponential divergences. Therefore it seems that this perturbative treatment might not be able to carry over in the case of the Frenkel-Kontorova lattice. However this is merely a preliminary result and thus certainly more detailed investigations are required in order to resolve that apparent discrepancy.

## 2.8 Stability Analysis of Kinks

One of the most important questions regarding the kink excitations is the one concerning their stability. In the discussion of the Peierls-Nabarro barrier both the numerical simulations of the form of the potential as well as in the full scale simulations we saw that there is a stable kink configuration centered on a lattice site as well as an unstable centered between lattice points.In this section we will present a mathematical method that can be used in order to prove the stability or instability of the kink configurations. We will discuss for simplicity the case of the 3 and the 4 point kink (i.e. a kink containing only 3 or 4 lattice sites) but the generalization of the method to any kink configuration will be straightforward.

The 3 point kink will contain 3 lattice sites on its "spine" therefore its configuration will be $(0, ..., 0, y_{i-1}, y_i, y_{i+1}, 0, ..., 0)$. Symmetry requires that $y_i = \pi$ and that $y_{i-1} = 2\pi - y_{i+1}$. Therefore the equation for $a = y_{i-1}$ will be (according to the F-K prescription) $2a + \frac{1}{d^2}\sin a = \pi$. However the reader will directly note the error in this calculation arising from the fact that the equation from the i-2 site will not hold true in this approximation (since $y_{i-1}$ will be the only nonzero term entering that equation and should thus be 0).However this is a general problem with the F-K prescription since if 2 points have zero ordinates then the same will be true for all sites. However discreteness can support kink solutions with only a few lattice sites. The reason for that can be easily seen to lie in the fact that for smaller d's the value of $y_{i-2}$ needed to satisfy the equation $y_{i-1} - 2y_{i-2} - \frac{1}{d^2}\sin(y_{i-2}) = 0$ is getting smaller and thus the 3 point approximation is of increasing accuracy as d decreases. The same of course holds true in the 4 point kink case. There the corresponding equations will be (again using symmetry) $(a, b, c, d) = (a, b, 2\pi - b, 2\pi - a)$ where a,b,c,d correspond to the ordinates of the sites i-2 , i-1 , i , i+1. The equations that a and b will satisfy are $2a - b + \frac{1}{d^2}\sin(a) = 0$ , $3b - a + \frac{1}{d^2}\sin(b) = 2\pi$

The mathematical method to detect the stability or instability of these kink solutions will be based on the Evans Function technique. This would therefore be a good point to introduce the mathematical machinery behind this technique.

### 2.8.1 Interlude IV : Evans Functions

The Evans function technique was originally introduced by Evans ([36]) in 1975 to study the stability of impulses in nerve axon models. However recently it has been used in a variety of other pattern forming systems in order to give information about the linear stability of localized solutions ([37-40]).

This technique in the case of the continuum (for PDE's )is described quite succintly in the appendix A of [40]. It is a method for detecting exponential instabilities. This method uses the linearization of the equation around the localized excitation and the behavior of the excitation close to the boundaries of the domain under study in order to find a constant coefficient operator that will describe the behavior close to the 2 boundaries. Assuming a solution of that type i.e. $\exp(\mu\xi)\exp(\lambda t)$ one can find the values of relation of $\mu$ w.r.t $\lambda$ by solving the eigenvalue problem

for the constant coefficient operators. Now starting ,say, at $-\infty$ with the eigenvalue that is nicely behaving in that boundary and "shooting" this solution numerically through the localised excitation one retrieves both the growing and the decaying mode at $+\infty$. Therefore the coefficient that multiplies the function that we started with (that will in the other boundary become the growing mode) has to be zero in order for this perturbation to the localised mode to "survive". This multiplying factor is the Evans Function $D(\lambda)$ and according to the above its zeros will yield the exponential instabilities to the mode under study. One other point that Pego et al. ([38-39]) proved is that the asymptotically $D(\lambda) \to 1$ as $|\lambda| \to \infty$. One nice way of visualising the existence of exponential instabilities through the zeros of the Evans Functions is by means of Nyquist plots.According to the argument principle the winding number of the imaginary axis around zero will yield (since $D(\lambda) \to 1$ as $|\lambda| \to \infty$) the number of zeros of D and thus of the unstable eigenmodes.The formal expression of this fact is given by the formula:

$$n_{windings} = -\frac{1}{2\pi} \int_{-\infty}^{\infty} \frac{D'(i\lambda)}{D(i\lambda)} d\lambda$$

Given these background notions we can now go on to apply this technique in the case of the 3 and 4 point kink.Notice that the lattice discrete version of the problem seems to be quite suitable for the use of this mathematical tool since the differential equation now becomes a matrix equation and the solution of the corresponding matrix eigenvalue problem will determine the stability of the localised modes.

Considering the F-K model ansatz $y_i = u_i + q_i$ where $u_i$ is the 3 or 4 point kink and $q_i$ is the perturbation around that localised solution.Then the linearised equation that $q_i$ will satisfy will read :

$$\ddot{q_i} = \Delta_2 q_i - \frac{1}{d^2} \cos(u_i)(q_i)$$

Using the functional form $r^i \exp(\lambda t)$ for the perturbation one obtains in the left far end (away from the localised solution) the equation $r + (1/r) = x$ where $x = 2 + \frac{1}{d^2} + \lambda^2$.Thus $r = \frac{x \pm \sqrt{x^2-4}}{2}$. Starting off at this end with the nicely behaving solution (according to the value of $\lambda$ it could be the one with the plus or with the minus sign -whichever of the 2 has $|r| < 1$) .Let us denote the solution of the binomial with $|r| > 1 \to r$ whereas the one with $|r| > 1$ we denote by $r_1$.

Now separating the 2 subcases in the 3 point kink at the lattice sites (-1,0,1) one can shoot this solution down to i=-2 obtaining that the site i=-2 has $q_{-2} = r^{-2} \exp(\lambda t)$ and $q_{-1} = r^{-1} \exp(\lambda t)$ .Now solving through the kink and using the notation $a_1 = 2 + (1/d)^2 cos(a)$ and $a_2 = 2 - (1/d)^2$ one obtains for the lattice sites 0,1,2 :$q_0 = (\lambda^2 + a_1) r^{-1} + r^{-2}$, $q_1 = (\lambda^2 + a_2) q_0 - q_{-1})$ ,$q_2 = (\lambda^2 + a_1) q_1 - q_0$ . Then since $q_3 = x q_2 - q_1$ one has an expression for say $q_2, q_3$ which are to the right of the kink. On the other hand from the Evans function theory these points should have the spatial dependence $q_2 = Ar^2 + B{r_1}^2$ and $q_3 = Ar^3 + B{r_1}^3$. The coefficient A of the growing mode (the one depending on r) yields the Evans function as $D(\lambda) = \frac{{r_1}^2}{\sqrt{x^2-4}}[r_1 q_3 - q_2]$.The plot of the real valued function D as a function of the eigenvalue ($D(\lambda)$) is given in figure [23] for various values of the parameter d(this is given as a 3 dimensional plot for different values of d but for reasons of comparison and consistency it will be presented here rather than in the end of the text). The single zero in the cases of low discreteness where our solution of a 3 point kink can be supported by the lattice yields the instability of that mode as we had intuitvely predicted before.In the complex plane one can plot $D(i\lambda)$ as shown in figure [24] (for d=0.75). The branch cuts of the discrete case linearised spectrum ( the phonon band) lie in the imaginary axis of the spectral plane and thus closing the contour on the right half plane one clearly can get the Nyquist plot of the Evans function and the single enclosure clearly indicates the unstable mode of the 3 point kink. Another rather technical point is the fact that instead of the function $\sqrt{(x^2-4)}$ that introduces undesirable branchcuts in the complex plane one can normalise the function $r_1 q_3 - q_2$ which is the function whose zeros are of interest with the appropriate power of r (or $r_1$) since neither introduces any extra zeros (their product is always 1).Thus we used ${r_1}^3$ as normalisation to the above function.

The same procedure carries over in the case of the 4 point kink .There one can go down to the site -3 by shooting the solution of the left end which results in $q_{-3} = r^{-3} \exp(\lambda t)$ and $q_{-2} = r^{-2} \exp(\lambda t)$.Then again defining $a_1 = 2 + (1/d)^2 \cos(a)$ and $a_2 = 2 + (1/d)^2 \cos(b)$ one obtains for the sites -1,0,1,2 (their spatial dependence): $q_{-1} = (\lambda^2 + a_1) r^{-2} - r^{-3}$ , $q_0 = (\lambda^2 + a_2) q_{-1} - r^{-2}$ , $q_1 = (\lambda^2 + a_2) q_0 - q_{-1}$, $q_2 = (\lambda^2 + a_1) q_1 - q_0$. Again using the formula for the real $D(\lambda)$ (i.e. with $\lambda^2$ instead of $-\lambda^2$ in the formulas) one obtains ,for various values of the discreteness parameter d, the graph shown in the figure [25].Thus in this case the Evans function appears to have

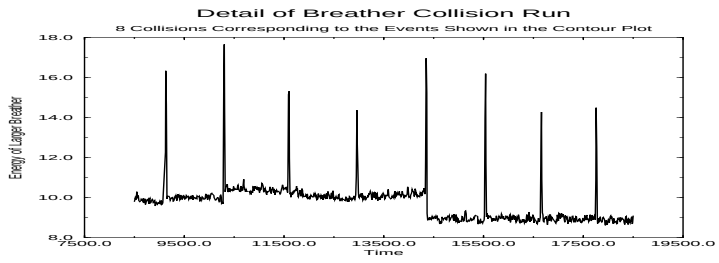


Figure 44: Detail of Breather Collision Run Corresponding to the Contour Plot Given Below

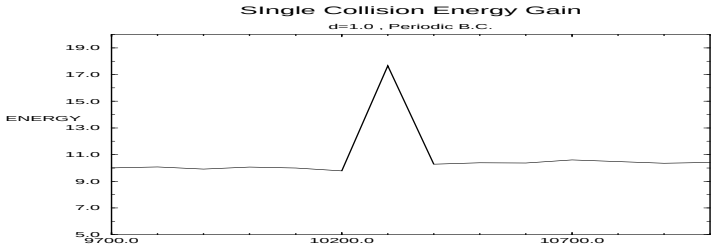


Figure 45: Single Collision Energy Gain(for the Larger Breather)

no zeros.One can verify this statement from the Nyquist plot of the figure [26] (for d=0.75) in the complex spectral plane where no enclosures of the origin are found in closing the contour and thus the 4 point kink is stable as was anticipated.

The physics behind the existence or non-existence of a zero of the Evans function in the 2 cases can be understood by means of the bifurcation of the GoldStone mode frequency in the spectral plane in the 2 cases.In the 3 point kink the mode eigenfrequency bifurcates in two real frequencies in the spectral plane one of which is producing a growing and one a decaying mode.Thus closing the contour of the plane the Evans function technique traces out this frequency and indeed if one finds the eigenmode related to the value of $\lambda$ for which D=0 one obtains a graph shown in the figure [27] which is a clearly related to the GoldStone mode. On the other hand in the 4 point kink case the bifurcation occurs along the imaginary axis of the spectral plane and thus the contour integration does not pick up a zero since the mode is in this case stable. Incidentally a quite direct way to identify eigenmodes of the system is to use a newton iteration for finding the zeros of D with a good initial guess for the eigenvalue. Using that technique one can pick up not only the GoldStone mode but also other interesting modes such as the shape mode of the kink discussed before (as shown in figure [28] showing the graph of the eigenmode corresponding to the second zero of D along the imaginary axis).

The study of stability given above concludes our discussion of the properties of the single 2 $\pi$ kink of the Discrete SG equation. In the next section the properties of kink-kink and kink-antikink interactions will be discussed via numerical simulations and an attempt to explore the existing theories and their limitations will be given.

# 3 Kink Interactions

1. Kink-Kink Interactions

   A very simplistic qualitative model in order to study kink-kink interactions was originally introduced in [15].There, Peyrard and Kruskal in their effort to analyze the properties of higher order kinks such as the 4 $\pi$ kink (which will be discussed in the next section more extensively) considered this entity, which as we will see is not a solution of the equation but which however is supported on the lattice due to discreteness, as composed by 2 2 $\pi$ kinks. Then the behavior of this entity could according to them be studied with a simple qualitative model containing the standard repulsive interaction between continuum solitons and the

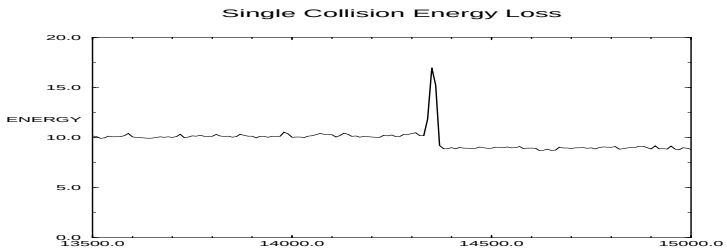


Figure 46: Single Collision Energy Loss (for the Larger Breather)

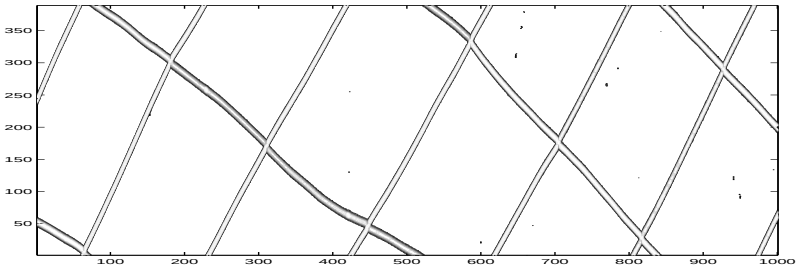


Figure 47: Breather Energy Contour Plot: No Generic Evidence for Significant Energy Gain of Larger Breather Energy at the Expense of the Smaller One Seems to be Present

Peierls-Nabarro barrier due to lattice discreteness.Thus their equation for the position of the 4 $\pi$ kink was:

$$m\frac{d^2r}{dt^2} = 2kr - 2\pi E_{P-N}\cos(\pi vt)\sin(\pi r)$$

where m is the mass of each soliton and the first and second term on the RHS are justified by the physical principles mentioned above. The fact that such a simple model captures some of the qualitative characteristics (for large $v_0$ bounded oscillatory solution corrsponding to a stable 4 $\pi$ kink whereas for small $v_0$ unbound r and thus unstable 4 $\pi$ kink) of the kink interaction picture is quite helpful. However it is understandable that a more complete numerical investigation of the kink-kink interactions as well as a more complete theory with stronger quantitative predictive power would be desirable.

For that purpose we set out to numerically investigate the possible outcomes of kink-kink collisions in the Frenkel-Kontorova model. Our numerical simulations cover a range of discreteness parameters as well as a range of relative velocities of the kinks. For that reason we present the results in the form of a phase diagram over the parameter space. The x-axis of our graph represents the difference in velocities of the 2 kinks in the numerical experiment whereas y yields the values of the corresponding discreteness parameter d.The perceptive reader might note that apart from these 2 important factors there is a 3rd one which involves the initial distance between the kinks. We will refer to this parameter briefly in the end of this section.

The results of our experiment indicate that there is quite rich dynamics occuring in the k-k interactions. As one can see the experiments (shown in figure [29]) were run for 3 different values of he discreteness parameter (d=1.15,1.0,0.85-the single 2 $\pi$ kinks in the discrete lattice get pinned at d=0.75) and for 3 different values of velocity difference. The bigger velocity was always 0.8 and the smaller varied between 0.5, 0.3, 0.1. For large value of the discreteness parameter (1.15) one sees that solitons behave in a particle like manner as we expect continuum solitons to behave.This is to be expected since for $d > 1.0$ the effects of discreteness become weaker (even though they are still present). Therefore for $v_{smaller} = 0.1$ the kink with the bigger velocity will have enough time to catch up with the smaller one and the collision will cause an exchange of velocities (as is expected for particles of the same mass).This is shown both in terms of a space time plot of the position of the 2 kinks (figure [30]) as well as in the 3 dimensional full time evolution of the configuration ([$3d_2$]). In the other 2 cases the kink with the smaller velocity is moving sufficiently fast that the kinks will not collide before the collision of the one of the smaller velocity with the boundary which reverses its direction.Once

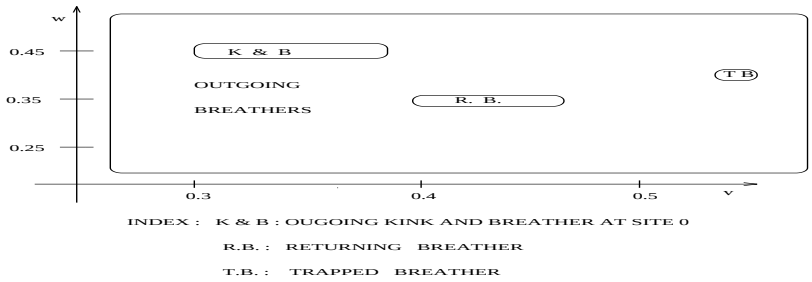


Figure 48: Parameter Space Phase Diagram for Breather-Image Collision Potential Outcomes

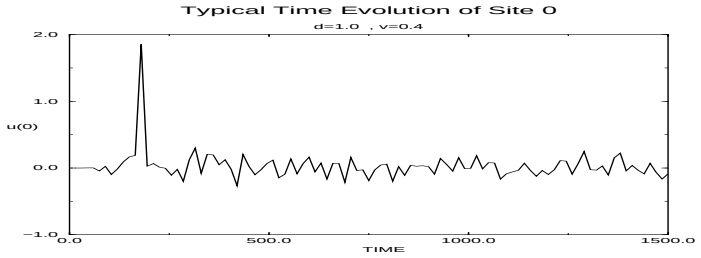


Figure 49: Typical Site [0] Time Evolution for Single Breather-Image Collision

again , though, the collision will result in particle-like velocity exchange. For smaller values of the discreteness parameter more interesting phenomena appear. In the case i.e. of d=1.0 for $v_{smaller} = 0.3, 0.5$ the large kink gradually decelerates and after a transient period the 2 kinks propagate in a constant velocity configuration resembling a propagating double SG kink. However what is even more striking is the behavior of the larger kink in the case of $v_{smaller} = 0.1$.In that situation the kink with the larger velocity despite its initial velocity to the right feeling the effect of discreteness and of the slowly propagating second kink,after the collision, prefers to reverse its velocity and to propagate in the opposite direction. this appears as a quite remarkable result. A similar phenomenon was reported in the case of the $\phi^4$ model in [25] for the single kink case but in our discrete Sine-Gordon as well as $\phi^4$ simulations we have never observed such spontaneous direction reversal for a single kink. However the above mentioned influence of both the kink-kink interaction and the radiation field seem to be able to produce a reversal of the kink direction of propagation. This result is again shown in a space time plot of the position of the 2 kinks to help visualization (figure [31]). Further lowering of the value of d results in pinned configurations (after, possibly, some transient motion) resembling a static double Sine-Gordon kink. This completes our numerical description of the possibilities arising in the cases of discrete Sine-Gordon kink interactions. Now let us proceed to discuss the $k - \bar{k}$ collisions in the same manner.

2. Kink-Antikink Interactions

   The wealth of behavior arising in Kink-Antikink collisions even for continuum versions of soliton containing models had been appreciated as early as 1983 ([41]).In that seminal work Campbell et al. investigated numerically the continuum kink-antikink interactions finding that soliton-antisoliton interactions in the SG equation demonstrate only conventional integrable systems' solitonic behavior passing through each other "unscathed". However the non-integrable nature of the $\phi^4$ theory does not permit the solitons to pass through each other . Therefore the solitons in that case have to be reflected off each other with a final velocity different than the initial one. Furthermore the fact that the region between the kinks is not at a minimum of the potential energy V creates in this case also the possibility for complete $k - \bar{k}$ annihilation in radiation (phonons) as well as for the formation of long-lived breathing bound final states.

   However our numerical investigations (which agree with the results of [41] in the large d limit (approaching the continuum) indicate that the kink-antikink collisions in the discrete Sine-Gordon have a much broader band of potential resulting states. We again present our results in a parameter space type of phase diagram of discreteness parameter .vs. difference in velocity (as is shown in figure [32]). The large velocity (k) is set again to 0.8 and the smaller one ($\bar{k}$) is given the values -0.1,-0.5,-0.7,-0.8 for discreteness values of d=1.15, 1.0, 0.85.

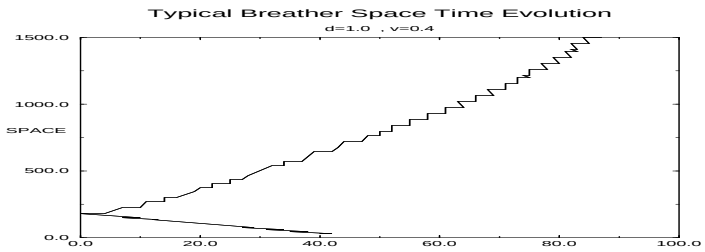


Figure 50: Typical Space Time Plot of the Breather Position for a Single Breather-Image Collision

What we found is that for large values of the discreteness parameter and for large velocities of the kink and the anti-kink the generic behavior closely matches that of the continuum counterpart (i.e. for d=1.15 and $v_{smaller} = 0.1, 0.5, 0.7, 0.8$ or for d=1.0 and $v_{smaller} = 0.8$). That is the kink and the antikink pass through each with a mere phase shift and without being reflected. The corresponding simulation results are shown in figures [33] (which gives a space time plot of the distance between the 2 kinks -also compared with the theoretical predictions that will be introduced below) and [$3d_3$] (a 3 dimensional picture of the $k, \bar{k}$ pair as they go through each other). For smaller d (1.0) discreteness becomes more significant in determining the final state and the experiments indicate that for all 3 cases (v=0.1,0.5,0.7) a breather long-lived oscillating state will form. The same is true for even lower values of d (0.85) in which in 3 of the 4 sub-cases ($v_{smaller} = 0.5, 0.7, 0.8$) again a breathing state is the outcome of the collision. However in the fourth case a bound state of a pinned kink-antikink pair settles down as the final state of the lattice( as can be seen in figure [34]). The perceptive reader will immediately note that as opposed to the case of kink-kink collision in the $k - \bar{k}$ case even for small d the configuration seems to have enough energy to move rather than to get pinned in a static final state. It is important to note however that in the case of low velocities of the antikink a number of interesting phenomena occurs to the breather resulting from the collision. For example when d=0.85 and $v_{\bar{k}} = 0.5$ the breather forms and then moves in the opposite direction to the one of the fast moving kink. More impressively for the case of d=1.0 and $v_{\bar{k}} = 0.1$ one finds that the resulting breather appears to be moving for some time in the one direction and then it seems to be stopping at a certain point wherein it oscillates for a while and then it decides to move in the opposite direction (i.e. see figure [$3d_4$]). As one can easily conclude the above phenomena constitute an extreme wealth of possible behaviors of the collisional outcome and seem to indicate that these possibilities might not be analytically tractable. However one would like to know what fraction of this behavior it might be possible to capture in an analytical model. Let us therefore proceed to the next subsection where we discuss more extensively the models existing in the bibliography and their range of applicability.

### 3.0.2 Models of Kink(-Antikink) Interactions

Since we gave a brief discussion of the Peyrard and Kruskal argument in the case of kink-kink interactions we will focus in the section in the study of the existing models for kink-antikink interactions.

One of course is tempted to extend the Peyrard and Kruskal approach for the $k - \bar{k}$ case where the repulsive k-k interaction is just converted to an attractive $k - \bar{k}$ interaction yielding an equation for the distance between the sub-kinks of (in this case) the breather state that these subkinks can form as an outocme of the collision:

$$m\frac{d^2r}{dt^2} = -2kr - 2\pi E_{P-N}\cos(\pi vt)\sin(\pi r)$$

In this case for low velocity one retrieves an oscillating in time stable configuration that corresponds to the breather is shown in the figure [41]) whereas for large values of the initial velocity (which can be thought of as a measure of the difference of velocities of the initial subkinks) the configuration will be unstable yielding the well known separation of $k - \bar{k}$ going through each other. However in view of the existence of a phenomenological undetermined parameter k in the model which should obviously (according to our numerical findings) be dependent on d in a complicated way one would appreciate a more natural and clear way of determining the behavior of the system.

When discussing the case of the single kink both in terms of the Peierls-Nabarro barrier as well as in terms of the radiative effects arising from the single kink we saw that the BWS theory was quite capable of predicting these effects of single kink dynamics. Therefore one of the main challenges and questions clearly concerns the possibility of extending such a collective variable theory for case of solitonic interactions on a discrete lattice.

The generic motivation for collective variable theories in the continuum non-linear Klein-Gordon type of equations arises from the fact that variables such as the kink position can not be treated by linearly superposing the corresponding eigenfunction with the kink itself since the resulting secularity would create terms growing in time and thus perturbation theory would fail and quantum fluctuation theory would yield unbounded fluctuations. Thus one has to introduce a new time-dependent coordinate in the problem (the kink position) in order to remove any undesirable secularities and/or unbounded fluctuations.

Therefore one can try to apply the collective variable technique developed by BWS in order to study more than one kinks (and/or antikinks). The generalization can be performed in the following way. Suppose a kink and an antikink (the changes for a k-k system will be obvious) given by the continuum ansatz $f = 4\arctan(\exp(k(i - X_1)))$ for the kink and $g = -4\arctan(\exp(k(i - X_2)))$ for the antikink whereas $q_i$ describes the radiation field. Then our resulting ansatz for the problem will be $y_i = f_i + g_i + q_i$. Direct substitution of this ansatz in the F-K equation results in one equation which can be used once we know the kink's $X, \dot{X}, \ddot{X}$ in order to determine the radiation field. This equation reads:

$$\ddot{q_i} + \ddot{X_1} f'_i + \dot{X_1}^2 f''_i + \ddot{X_2} g'_i + \dot{X_2}^2 g''_i = -\frac{1}{d^2}\sin(f+g+q)_i + \Delta_2(f+g+q)_i$$

As is obvious now the system has 2 N +4 variables since the collective variables $X_1, X_2$ and the corresponding momenta introduce an extra 4 unknowns. Therefore one has to impose according to the theory the 4 additional constraints : $< f'|q >= 0$, $< f'|p >= 0$, $< g'|q >= 0$, $< g'|p >= 0$. Now using the projection operator approach which is fully equivalent to the Dirac constraint dynamics theory one can act with the operators $< f'|$ and $< g'|$ on the equation above to project on the space of contraints and thus to obtain the system of equations for the dynamical evolution of the collective variables (using also the lemmas : $< f'|\ddot{q} >= -\ddot{X_1} < f''|q > -\dot{X_1}^2 < f'''|q > -2\dot{X_1} < f''|\dot{q} >$, $< g'|\ddot{q} >= -\ddot{X_2} < g''|q > -\dot{X_2}^2 < g'''|q > -2\dot{X_2} < g''|\dot{q} >$ which arise from double time differentiation of the constraints):

$$\mathbf{M}\ddot{\mathbf{X}} = \mathbf{F}$$

where $\ddot{\mathbf{X}} = \begin{pmatrix} \ddot{X_1} \\ \dot{X_2} \end{pmatrix}$, $\mathbf{F} = \begin{pmatrix} F_1 \\ F_2 \end{pmatrix}$ and $\mathbf{M}$ is the mass matrix:

$$\begin{pmatrix} M_{11} & M_{12} \\ M_{12} & M_{22} \end{pmatrix}$$

where $M_{11} =< f'|f' > - < f''|q >$ , $M_{12} =< f'|g' >$, $M_{22} =< g'|g' > - < g''|q >$ ,

$$F_1 = -\dot{X_1}^2(< f'|f'' > - < f'''|q >) + 2\dot{X_1} < f''|\dot{q} > -\dot{X_2}^2 < f'|g'' >$$
$$-\frac{1}{d^2} < f'|\sin(f+g+q) > +\Delta_2 < f'|f+g+q >$$
$$F_2 = -\dot{X_2}^2(< g'|g'' > - < g'''|q >) + 2\dot{X_2} < g''|\dot{q} > -\dot{X_1}^2 < g'|f'' >$$
$$-\frac{1}{d^2} < g'|\sin(f+g+q) > +\Delta_2 < g'|f+g+q >$$

One can then in principle solve the coupled system of equations for the 2 collective coordinates together with the equation for the fluctuations at each lattice site. The advantage of this method, if it is successful, (over the performance of the full scale simulation) is the fact that it should yield an accurate estimate of the behavior of the collective dynamical variables (i.e. the positions of the kink and the antikink or of the 2 kinks). Apart from that one still solves a system of 400 coupled second order ODE's (in fact 402)!

By performing the numerical simulation and the comparison with the integration of the full system one reaches the following conclusions (by viewing the results shown in the figure [35] -showing a comparison between the positions of the kinks in a space time plot as compared between the 2 collective variable BWS theory and the experiment-

- For short times with the kink and the antikink being far apart the theory follows quite closely the predictions of the experiment (in which the kink positions have been determined using the linear interpolation scheme mentioned in section 1). For these times the energy of the system is conserved to the 8th decimal digit and the typical values of the constraints are of the order of $1e^{-10}$.
- As time goes on and the solitons start to feel the presence of each other the positional prediction of the model becomes less accurate even though it can still be characterized as quite satisfactory (since also the typical standard deviation in the evaluation of the kink position can be considered to be around 1-2 lattice spacings).
- However as the kinks come even closer as is mentioned in [43] the BWS needs a very large amount of dressing in order to correctly describe the profile. As a result a numerical instability sets in the calculation of the 18 sums needed for the numerical integration at each of the 4 steps of the applied Runge-Kutta algorithm and thus one cannot predict by means of this approach the behavior of the kinks for very small distances.

Noting this potential difficulty (i.e. the need of strong dressing of the kink by means of the fluctuations) Boesch and Peyrard ([43]) proposed an alternative scheme for using the BWS theory with only one collective variable for this case study.

Their suggestion was based on the observation of the fact that the center of mass of this symmetric kink-antikink configuration (in the case of $k-\bar{k}$ having the same speed) will remain approximately constant in the time evolution of the $k-\bar{k}$ configuration. This assumption is strongly supported by their (and also by our) simulations of the F-K model. Therefore one can express the kink-antikink configuration in terms of a single collective variable z which describes the distance between the 2 solitons. Thus the BWS ansatz will read:

$$y_i = 4\arctan(\exp(k(i+z-X))) - 4\arctan(\exp(k(i-z-X))) + q_i$$

where now X is the fixed center of mass position of the $k-\bar{k}$ system (i.e. $X = \frac{X_1+X_2}{2}$ in terms of our previous notation) whereas $z = \frac{X_2-X_1}{2}$ is half the $k-\bar{k}$ distance. Following the same prescription as before and now naming f the 2 first terms of the expression for y given above one obtains (after similar algebraic manipulations as in the 2 C.V. case) the equations:

$$\ddot{z}(< f'|f' > - < f''|q >= \dot{z}^2(< f'''|q > - < f'|f'' >) + < f'|\Delta_2(f+q) >$$

$$-\frac{1}{d^2} < f'|\sin(f+q) >= 2\dot{z} < f''|\dot{q} >$$

$$\ddot{q}_i + \ddot{z}f'_i + \dot{z}^2 f''_i = -\frac{1}{d^2}\sin(f+q)_i + \Delta_2(f+q)_i$$

Therefore given this new set of coupled differential equations, which contains less sums and which has made use of the symmetry of the problem to split the dressing between the solitons, one can proceed to numerically integrate the model equations. The results of this attempt for the case of a kink-antikink collision in which each of the solitons has a speed of 0.3 and d=1.0 is shown in figure [33]. The initial value of $\dot{z}$ in the simulation was chosen so that the the theoretical and the model lattice have the same energy up to the 7th decimal digit. The maximum value of the constraints during the simulation was of the order of $1e^{-9}$ and the energy in both the model system and the original system was checked to be conserved to the 9th decimal digit. The comparison of the numerical experiment and of the model system yields the following conclusions:

- The model reproduces the behavior anticipated from the numerical experiment, namely, the solitons for this parameter set pass through each other un-reflected.
- While the solitons are far apart the prediction of the theory is in excellent agreement with the numerical simulation of the system.
- As the distance becomes very small there is a very small difference between the predictions of the 2 theories (barely visible in [39] and definitely justifiable within the range of accuracy of the prediction of the actual position of the kink and the antikink through the numerical intrerpolation scheme used in the experiment which is also increased when the distance of the pair is very small).

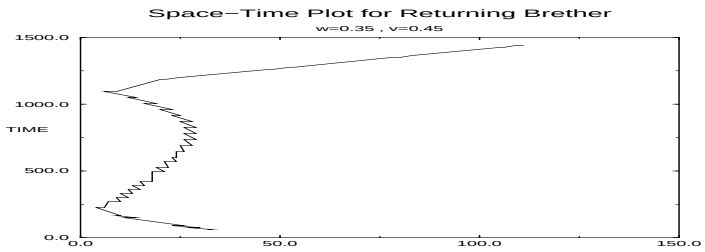


Figure 51: Space-Time Plot of Breather Returning Once to Collide With Its Image

- As the sub-kinks of the pair go through each other the prediction is ,again, virtually indiscernible from the actual numerical result of the integration of the F-K equations.

Therefore the above indicate that the BWS theory with one collective variable might be a quite handy tool in the effort to trace and understand in a more comlpete and quantitative way the behavior of kinks and antikinks (or kinks and kinks) in their interaction events. Along these lines for example one can position the useful conclusions of the study of the discreteness effects on the Sine-Gordon breather performed by Boesch and Peyrard in [43] (such as the result that the effective breather potential between $k - \bar{k}$ will be to completely cancel the Lorenz contraction due to the individual kink's motion. Of course more quantitative and more detailed studies required in order to compare the results of the BWS theory with the numerical experiments and also in order to extract more information about the individual behavior of the collective variables under the influence of the other kinks (antikinks ) present in the fsystem and also of the radiation field. Furthermore, there is an obvious need for appropriate extension of the BWS theory in asymmetric cases (i.e. cases where the individual collective variables of the pair start off with different velocities ) since most interesting dynamics phenomena appear in such collisional events. Future studies should address such comparisons in a more detailed way.

Another possible direction of future study could be the generalisation in the discrete case of the work of Hsu ([44]). This would involve the use of numerical computation of the time delay (advance) due to $s - \bar{s}$ $(s - s)$ interactions in order to derive the effective potential of the interaction by numerically solving the corresponding inverse problem.

Finally let us mention a few words about another parameter that is important in the problem, especially for small values of the discreteness parameters, namely the initial distance between the solitons. In principle the results of our simulations have been proved quite robust for sufficiently large distances between the initial solitons. However as the distance between the solitons becomes sufficiently small (in principle such that they feel each other in the initial configuration - a rule of thumb is that this is somewhere between 15-25 lattice sites since also the continuous solitons as seen above have a potential that decays as $32e^{-R}$ for $R >> 1$) many interesting phenomena arise. One such example is shown in the figures [36]-[37]. As our simulations indicate and as was established by Peyrard and Kruskal in [15] 2 $\pi$ F-K kinks get pinned by discreteness in the P-N barrier for $d = 0.75$. Therefore if we put 2 kinks at ,say , the lattice sites 190 and 210 at d=0.75 nothing will happen but if we put them at the sites 195-205 then for d=0.785 a "pinned implosion" occurs and the configuration goes to a $-2\pi$ to 0 kink-antikink system. And more impressively if one goes to even lower values of d such as d=0.697 one obtains moving breathers in the case where each individual kink would be trapped in the P-N barrier, being unable to move. Therefore the bound state lowers its P-N barrier by forming a breather and subsequently is able to move! Therefore one can see from these examples that small initial distances can substantially influence the dynamics of the problem. In principle however one would like to restrain oneself to larger initial distances and thereafter obtain a deeper understanding of the interplay of the important factors (kink interactions, radiation and P-N barrier) in an effort to understand more about the ways in which discreteness modifies the well understood continuum behavior of systems of solitonic excitations.

As is obvious from all the above the subject of dynamical interactions between solitons of the kink type in discrete lattices even in 1-d is extremely complicated and deserves further analytical investigations in order to provide explanations for the numerical findings reported in this paper.

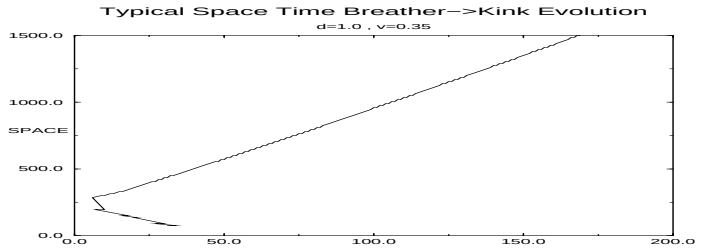


Figure 52: Space-Plot of Breather → Kink Evolution (notice the characteristic wobbling of the kink position)

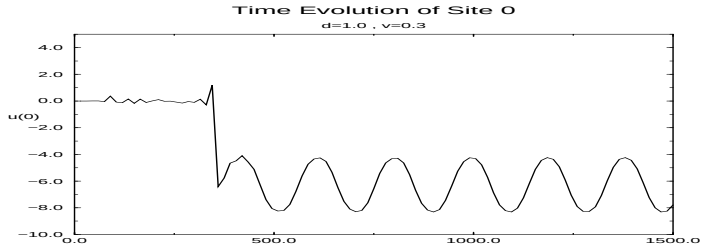


Figure 53: Zeroth Site Time Evolution Showing Fast Oscillations for v=0.3

# 4 4 , 6 , 8 $\pi$ Kinks

One of the most remarkable findings of the original work of Peyrard and Kruskal ([15]) studying the discrete Sine-Gordon equation was the existence of entities such as the 4 $\pi$ kink and the 6 $\pi$ kink that could propagate with a quite high velocity through the lattice being almost exact solutions with very small radiation in their wake. The reason why this is such an unexpected finding is that these "higher order" kinks (an example of which is shown in figure [38]- which depicts different snapshots of the spatial profile of a $6\pi$ kink) are not exact solutions of the continuum equation. As one can easily figure out from the form of the Sine-Gordon potential the permitted heteroclinic connections are from one maximum of the potential to the next. Given the fact that the maxima lie at $2n\pi$ one cannot overshoot the maximum at $2\pi$ in order to obtain an heteroclinic connection between 0 and 4 $\pi$. Furthermore direct substitution of the of the $2n\pi$ kink solution defined as $y_{2n\pi} = ny_{2\pi}$ in the continuum Sine-Gordon equation demonstrates directly due to the sinusoidal non-linearity that this cannot be a solution of the continuum equation. However considering the sine term one has i.e. for the 4 $\pi$ kink $\sin(8\arctan(\exp(x))) = 2\sin(4\arctan(\exp(x)))\cos(4\arctan(\exp(x)))$ whereas the other terms in the equation are simply multiplied by a factor of 2. Hence one can see why discreteness can keep together such a kink since if this kink is very steep (i.e. has very few points on its "spine" as will be the case for small d) for almost all of its points it will be true that the cosine term will be very close to 1 and thus the kink will be a good approximate solution of the continuum problems which will ,hence, be supported by the lattice. What Peyrard and Kruskal were also the first to appreciate was the fact that even though 2 $\pi$ kinks get pinned for d as high as 0.75 , $4\pi$ or $6\pi$ kinks can propagate on the lattice for much smaller values of d. Therefore our numerical investigation of this problem aimed at the identification of the curve illustrating the pinning-depinning transition. Our numerical findings are summarized in figure [39]. We found that in good agreement with the result presented in [15] 4 $\pi$ kinks can propagate for values of discreteness as low as 0.458 before getting pinned by the lattice. As one goes to higher order kinks the possibility of propagation extends to 0.3941 for 6 $\pi$ kinks and to 0.3529 for the 8 $\pi$ kinks. One can trace this pinning-depinning transition with a phase diagram such as the one shown in [39] (the drawing of a line is not permitted in principle since there are no other heteroclinic connections between the points but the dashed line is drawn to help the reader separate between the regions where pinning occurs from the ones in which the kinks can propagate). This diagram is strongly reminiscent of pinning-depinning phase diagrams in the case of propagation of fluid particles inside a porous medium with a random field of scatterers where the parameter corresponding to d is the angle of incidence of the fluid particles in the field and physical quantity corresponding to the kink amplitude is

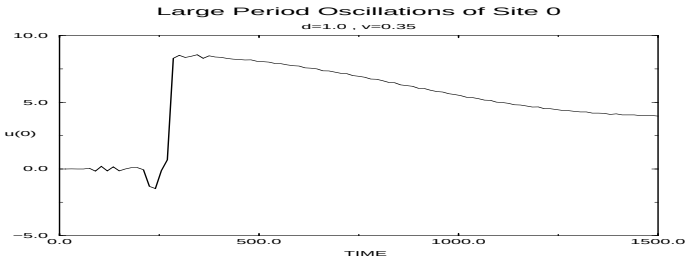


Figure 54: Same as Above but for v=0.35 Showing Long Period Oscillations

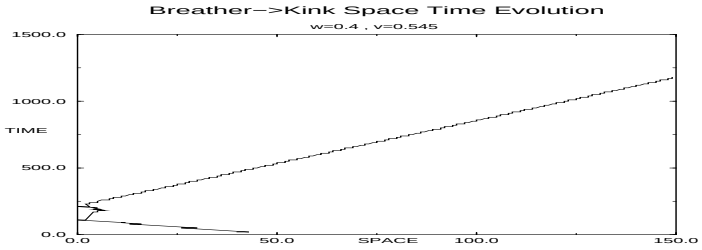


Figure 55: Kink Forming Breather Image Collision Just Prior to Trapping (w=0.4,v=0.545)

the pressure of the fluid (see i.e. [45]-[46]). This analogy which is rendered quite clear by direct comparison of our phase diagram with ,i.e., the figure [10.8] of [45]

We then went on to investigate more carefully the behavior of the 4 $\pi$ kink by means of numerical simulations. We constructed for this case also a phase diagram of a similar structure to the ones presented for the problem of kink interactions (since after all one can think of the 4 $\pi$ kink as composed by 2 $2\pi$ subkinks). The diagram of d .vs. 4 $\pi$ kink velocity is shown in the figure [40]. What one sees that in accordance also with the findings of [15] 4 $\pi$ kinks can propagate only at very high velocities of about 0.8. Propagation of a kink with that velocity was found for all 3 values of d for which the simulation was performed (d=1.0,0.75,0.5). For lower values of the velocity though (v=0.45) only the case of d=0.75 was found to result in a moving kink held together by discreteness. On the contrary for high d (d=1.0) the kink was found to breakup in 2 propagating 2 $\pi$ subkinks whereas very discrete lattices resulted in a bound state (static configuration of the 2 sub-kinks similar to the static kink of the double SG equation). For even lower values of there was no d for which the lattice could support the full 4 $\pi$ kink. Thus for d=1.0 the 2 subkinks propagated moving in a very complicated way as shown in figure [41] (a space time plot of the long time evolution of the 2 separating sub-kinks), whereas again lower values of d for which the individual sub-kinks are expected to be pinned resulted in static configurations similar to the ones mentioned above. These findings lead to the following conclusions:

- For high velocity we retrieve the results of [15] according to which high speed propagation of "higher order" kinks is possible in the discrete lattice with a very small radiation wake despite the fact that they are not exact solutions of the continuum equation.
- For lower velocities and high values of the discreteness parameters one retrieves the extremely complicated dynamics of interacting sub-kinks whose current quantitative understanding is far from being complete.
- For lower values of the velocity and high discreteness on the one hand the 4 $\pi$ kink cannot propagate (since it does not have enough energy) whereas on the other hand the individual sub-kinks should be pinned but also repel each other and therefore the resulting static configuration consists of 2 individual pinned kinks at an equilibrium distance from each other.

Let us note however at this point and in conjunction with the question raised in [15] on whether it is possible for 2 $2\pi$ kinks that are initially separated to form a 4 $\pi$ kink and subsequently propagate through the lattice, that

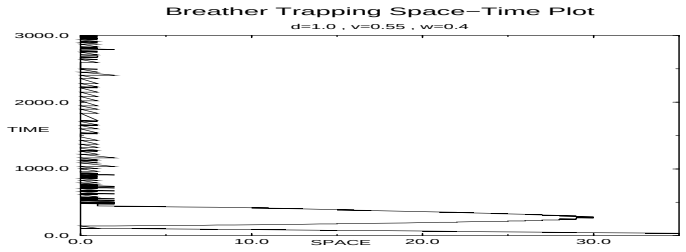


Figure 56: Trapping of Breather from Its Image : w=0.4, v=0.55

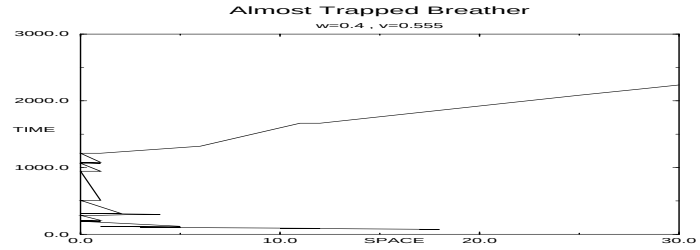


Figure 57: Almost Trapped Breather Right After the Trapping Stage:w=0.4,v=0.555

we have performed a large number of numerical experiments concerning that possibility. In none of the cases, not even in the most discrete ones (where it might seem preferable to form a $4\pi$ kink and propagate whence the 2 $\pi$ kinks are pinned by discreteness), were we able to trace such a formation. Independently of how close they initially were the 2 $\pi$ sub-kinks would prefer to stay pinned rather than form a higher order kink and propagate. This numerical observation for a wide range of parameters (v,d) as well as various initial distances, responds to the issue first mentioned by the authors of [15].This discussion of the behavior of "higher order" kinks, that constitute another intrinsic property of the discrete lattice, concludes our description of the behavior of kink solutions of the F-K model.

However all these inherent manifestations of discreteness render obvious the fact that numerical schemes such as finite difference and/or finite element techniques using direct discretizations of the lattice in obtaining ,for example, the finite difference stensils would pick up a number of phenomena that are absent in the continuum case. Therefore one is led immediately to the question of what would be the appropriate discretization for the study of the continuum Sine-Gordon or of the continuum $\phi^4$ equation. This question is answered in the following last section on the characteristics of kink solutions.

# 5 Proper Discretizations of the Continuum Klein-Gordon Equations

In order to describe discretizations of the continuum non-linear Klein-Gordon equations we will use the notion of Bogomol'nyi bounds introduced by Bogomol'nyi in 1976 ([48]) in order to obtain topologically stable solutions.

### 5.0.3 Interlude V: Bogomol'nyi Bounds

Our simulations for this particular problem were performed in the $\phi^4$ system therefore we will present the method as it was introduced in 2 papers by Speight and Ward and by Speight ([49]-[50]) examining it in parallel for the $\phi^4$ and for the Sine Gordon and we will then go on to give our own extension of the method to the Double SG case.

The time evolution of the continuum Sine-Gordon and $\phi^4$ models is governed by a Lagrangian $L = E_k - E_p$ where the kinetic energy in both cases is : $E_k = \int_{-\infty}^{\infty} dx\dot{\phi}^2$ whereas the potential is: $E_{p_{SG}} = \int_{-\infty}^{\infty}[(1/4)(\psi_x)^2 + \sin^2\psi)]dx$ and $E_{p_{\phi^4}} = \int_{-\infty}^{\infty}(\frac{1}{2}{\phi_x}^2 + \frac{1}{8}(1-\phi^2)^2)$ in the S-G (in which $\psi = (1/2)\phi$ is used) and $\phi^4$ models respectively.

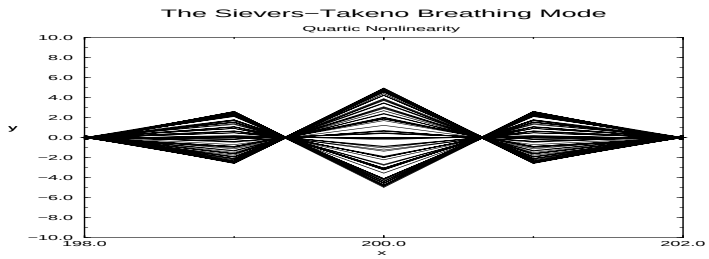


Figure 58: Sievers-Takeno Breathing Mode Stabilized by Quartic Anharmonicity

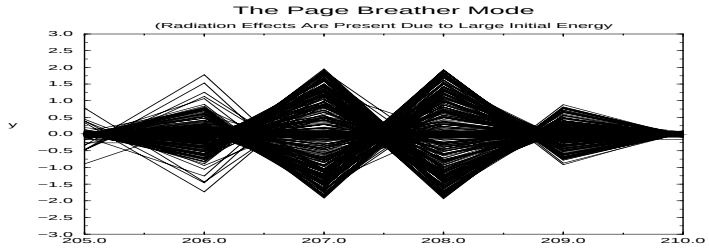


Figure 59: Page Breathing Mode "Surviving" in Quadratic Plus Quartic Potential

Since the moving kink is a minimum of the action functional in the case of the static kink not only will the action functional be time independent and equal to its value for the initial configuration but also the kinetic energy term will be absent. Therefore one immediately concludes that the static kinks will be minima of the potential energy. The Bogomol'nyi argument yields a convenient way of obtaining these minima. The argument goes as follows: For the Sine-Gordon equation the following inequality can be used : $0 \leq (1/4)\int_{-\infty}^{\infty}(\psi_x - \sin(\psi))^2 dx = E_p + (1/2)\int_{-\infty}^{\infty}(\partial_x(\cos\psi))dx = E_p - 1$ using the kink boundary conditions. Therefore according to the above argument the potential energy is bounded by 1 and this minimum value is obtained if $\psi_x = \sin\psi$ which yields the static continuum solution $\psi = 2\arctan(\exp(x - x_0))$ which can then be boosted in the solution of the full time dependent non-linear equation by means of a Lorenz transformation. The corresponding bound in the $\phi^4$ is obtained as follows: $0 \leq (1/2)\int_{-\infty}^{\infty} dx[\frac{d\phi}{dx} - (1/2)(1-\phi^2)]^2 = E_p - (1/2)\int_{-\infty}^{\infty}[\partial_x(\phi - \phi^3/3)]dx = E_p - (2/3)$ Therefore in that case $E_{p_{min}} = 2/3$ and this minimum is obtained for $\phi_x = (1/2)(1-\phi^2)$ which subsequently yields $\phi(x) = \tanh(1/2)(x-x_0)$ which again using the continuous symmetry of the Lorenz boost can be transformed to the full propagating kink solution of the time-dependent equation.

The problem with the conventional discretizations of these models, such as the 3 point finite difference stensil used to perform finite difference computations by substituting the second order derivative with the second order difference, is that they do not preserve this topological lower bound. Therefore this destroys the existence of exact static solutions (as well as the integrability of the problem) creating the entire new spectrum of phenomena encountered in the F-K model.

Therefore Ward's idea ([49]) was to seek a discrete version of the potential energy of the form :

$$E_p = \sum_i (1/2)D^2 + (1/8)F^2$$

such that in the continuum limit $D \to \phi_x$ and $F \to 2\sqrt{(}V)$ (even though normalization factors may vary for convenience according to the case under study) and also such that $DF = \Delta S.T.$ where S.T. denotes the surface terms as appearing in the continuum version of the Bogomol'nyi argument. If one is able to find such D,F then the Bogomol'nyi argument goes through in its discrete version i.e.: $0 \leq (h/2)\sum_i (D - (1/2)F)^2 = E_p - (h/2)\sum DF$ and now using the identity that the product of DF has been chosen to satisfy one retrieves the surface terms at the end points of the kink (thus from the kink boundary conditions the same term as in the continuum and the lower bound of $E_p$ is preserved.

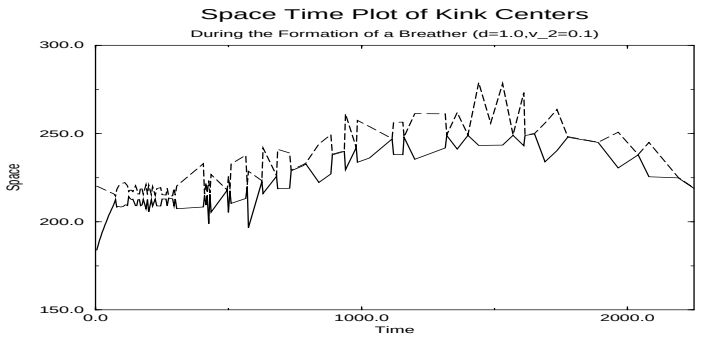


Figure 60: Kink-Antikink Breather Forming Collision in Space-Time Plot Corresponding to the Conditions of the 3d Plot of Figure:[$3d_4$]

Thus, now there will be a topologically stable exact static solution that will minimize the potential energy over the discrete lattice and which will be the solution of the first order difference equation $D = (1/2)F$.

Let us denote by $\phi_+$ the solution on the next lattice site from the one with ordinate $\phi$ ( following the notation of [49],[50]). As always in our study we will set h=1 (even though the authors of these 2 references study the equations for various possible values of h for simplicity we will set h=1 and the functional form of the solutions with $h \neq 1$ can be obtained by straightforward generalization). Then the main result of the above mentioned references is the finding of the most natural choice for the functional forms of D,F as functions of $\phi, \phi_+$. These will be : $D = 2\sin(1/2)(\psi_+ - \psi)$ and $F = \sin(1/2)(\psi_+ + \psi)$ for the S-G equation and $D = \phi_+ - \phi$ and $F = 1 - (1/3)({\phi_+}^2 + \phi_+\phi + \phi^2)$ for the $\phi^4$ model. Therefore using these choices for the spatial discretization of the potential energy one can build a discrete version of a continuum non-linear equation for computational purposes that:

- Has the proper continuum counterpart behavior
- Preserves the Bogomol'nyi argument for the discrete case and thus there exists a topologically stable minimum of the potential energy which will constitute an exact static solution of the discrete problem.

The main property of this static solution which can be found by means of the solution of the first order difference equation $D = (1/2)F$ will be that, given the fact that it's an absolute minimum of the potential energy it will not "feel" a P-N barrier due to discreteness in its propagation. All the above arguments indicate that this might be a good discretization for the counterpart continuum system since there will be no trapping phenomena and at the same time for low velocities such that the fundamental frequency associated with the kink is outside the phonon band (i.e. $v \simeq 0.157$ for $d = 1.0$) the radiative effects will be very small and coming only from higher order harmonics. Hence, the main expressions of the lattice discreteness will be absent and the system will be quite close to the continuum behavior. In the case of the Sine-Gordon equation Speight and Ward were able to find analytically the static solution mentioned above to be:

$$\psi = 2\arctan(\exp(k(x - X_0)))$$

where now $k = 2arctanh(1/2)$ (or $(2/h)arctanh(h/2)$ for lattice spacing h). In the case of the $\phi^4$ the more complicated nature of the Bogomol'nyi equation ${\phi_+}^2 + (6/h + \phi)\phi_+ + (\phi^2 - (6/h)\phi - 3) = 0$ necessitates the explicit construction from each point of the next solution point in the static minimum of $E_p$. Lorenz boosting of this static solution in each of the above cases or an initial continuum type kink solution is a good initial condition for the full scale coupled ODE's simulation. The set of coupled ODE's with the new (more appropriate) discretization introduced by the Bogomol' nyi considerations will have the following form in the 2 cases under study:
SG: $\ddot{\psi} = [\sin(\psi_+ - \psi) - \sin(\psi - \psi_-)] - (1/4)[\sin(\psi_+ + \psi) - \sin(\psi + \psi_-)]$

$\phi^4$: $\ddot{\phi} = \Delta_2\phi + (1/12)[(2\phi + \phi_-)(1 - (1/3)({\phi_+}^2 + \phi_+\phi + \phi^2)) + (2\phi + \phi_+)(1 - (1/3)({\phi_+}^2 + \phi_+\phi + \phi^2))$.
It is the simulation of this modified $\phi^4$ model that is demonstrated in figure [$3d_5$] (for original velocity of v=0.1 and

for an initial continuum kink profile). As is clearly demonstrated in the simulation after an original reshaping of the kink to a more appropriate velocity (since our solution is not an exact solution to the problem) the kink propagates with virtually no radiation effects and without feeling the effect of the Peierls-Nabarro barrier (no wobbling seems to be present as the kink passes through the lattice sites). These simulation results verify the theoretical prediction that the preservation of the topological lower bound and the consequent disappearance of the Peierls - Nabarro barrier can provide the proper discretizations of non-linear continuum Klein-Gordon equations. In fact this "prescription" in the case of the Sine-Gordon equation can be generalized (as was done in a subsequent paper by Zakrzewski ([51]) by replacing $\ddot{\psi} \to \frac{\ddot{\psi}}{1+a\dot{\psi}^2}$, $D \to aD$, $F \to F/a$ and choosing appropriate forms of f,a) in order for the model to possess time dependent solutions.

Given the significance of this prescription for the modelling of continuous systems we think it is worthwhile to give a similar application of the argument for the case of the Double Sine-Gordon equation. In that case the potential $V[\phi] = \lambda(1-\cos(\phi)) + (1/2)(1-\cos(2\phi))$ and is shown in figure [42]. As is discussed in [52] the potential has its minima at 0 (mod $2\pi$) and a local minimum at $\pi$ for $0 < \lambda < 2$ as is shown in the figure (that is drawn for $\lambda = 1$). The 2 free uncoupled $\pi$ kinks that are solutions at $\lambda = 0$ become weakly coupled for $0 < \lambda < 2$ and therefore the 2 $\pi$ kink splits in 2 separated $\pi$ subkinks. For $\lambda > 2$ the minimum at $\pi$ disappears but we are not going to be interested in that regime since in that case the 2 subkinks are indistinguishable yielding a 2 $\pi$ kink that is well understood within the context of the original Sine-Gordon model (and its modified version). Therefore in our case one can write the following equation for the bound:

$$0 \leq (1/2)\int(\phi_x - \sqrt{(}2V))^2 = \int_{-\infty}^{\infty}(\frac{{\phi_x}^2}{2} + V) - \int_{-\infty}^{\infty}\phi_x\sqrt{(}2V)$$

But the last integration can be performed explicitly:

$$\int_{-\infty}^{\infty}\phi_x\sqrt{(}2V) = 2(\cos[s/2]\sqrt{\frac{\lambda}{2} + (\cos(s/2))^2} + \frac{\lambda}{2}\log(\cos[s/2] + \sqrt{\frac{\lambda}{2} + (\cos(s/2))^2})$$

where s takes the values of the kink boundary positions at the endpoints 0 and 2 $\pi$ (the integral will obviously have a positive definite (since the integrated function is always $> 0$ in the interval) parameter dependent value which will be the topological lower bound of the potential energy $E_p$. Now one can pick as $D = \phi_+ - \phi$ and as $F = \frac{1}{\sqrt{2}}\frac{(\cos[s/2]\sqrt{\frac{\lambda}{2}+(\cos(s/2))^2}+\frac{\lambda}{2}\log(\cos[s/2]+\sqrt{\frac{\lambda}{2}+(\cos(s/2))^2})_{\phi}^{\phi_+}}{\phi_+ - \phi}$ which $\to \sqrt{V}$ in the continuum limit. Using these choices that preserve the Bogomol'nyi bound one can obtain the dicrete double Sine-Gordon exact static solving numerically the difference equation $D = \sqrt{2}F$. Starting from an initial value $\phi$ one can find all the subsequent points constituting the kink by finding each time the next root of the nonlinear difference equation through a Newton iteration. The results of this computation are shown in the figure [43] which represents the exact discrete static solution which can then be boosted and used as an initial condition for the time dependent problem. The proper discretization of the continuum equation can now be given as:$\ddot{\phi} = -\frac{\partial E_p}{\partial \phi}$ where $E_p = \sum_i \frac{D^2}{2} + F^2$.
This completes our discussion for the behavior of kinks in the non-linear Klein-Gordon lattices. Hereafter we will devote some space to the discussion of some open problems regarding another type of excitation arising both in the discrete and in the continuum version of these equations: the breather modes.

# 6 Breather Dynamics

Breathers as was briefly mentioned before (since they appeared as possible outcomes of F-K kink collisions) are exponentially localised in space and oscillating in time solutions of the continuum as well as of the discrete non-linear Klein-Gordon equations.

For example in the case of the Sine-Gordon equation the form of the continuum breather is well known to be:

$$\phi_b = 4\arctan(\frac{\sqrt{(}1-w^2)}{w}\frac{\sin(w\gamma(t-vx))}{\cosh(\gamma\sqrt{(1-w^2)}(x-vt))})$$

As is highlighted in [12] (which incidentally is a very good introductory textbook to the world of solitons with a plethora of physical applications demonstrating the increasing physical significance of solitonic excitations) the

importance of such a solution lies in the fact that its rest energy is:

$$E_b = 16\sqrt{(1-w^2)}$$

which is clearly less than the rest mass of the 2 solitons from which the breather may arise (as we saw in our numerical investigation of kink interactions). Therefore this energy can vary from 16 to 0 according to the frequency of the resulting breather and hence even small amounts of energy are able to excite breather modes in the model. That is why especially at high discreteness, where the solitons are strongly affected by the effects of the lattice and thus are no longer continuum solitons they seem to prefer to form breather modes rather than to follow the conventional continuum soliton behavior.

The rigorous argument for the existence of these modes in the case of Hamiltonian networks of coupled oscillators was originally given in a very interesting paper by Mackay and Aubry ([53]). Their method essentially involved the extension of the so-called anti-continuum limit. This is the limit of the uncoupled oscillators where it is known that localised oscillatory excitations exist. Their argument for the proof in the case of weak coupling between oscillators was based on the fact that for non-resonant (with phonons) , anharmonic (frequency should be amplitude dependent) oscillations one can use the implicit function theorem (for a certain operator whose zeros are periodic orbits of the problem) to obtain a locally unique continuation of a periodic orbit of the same period as the original oscillation of the single oscillator. Using more elaborate operator theory techniques they were able to establish also the exponential decay of these oscillating solutions and thus their breather mode nature. In fact in a subsequent paper Marin and Aubry([54]) were able to quantify that argument in order to obtain breather solutions and even to extend it in systems without an explicit anticontinuum limit (such as FPU chains).

Over the last few years there has been a very strong effort of the scientific community in order to obtain a deeper and more quantitative understanding of these breather modes.This effort has been triggered in part from the importance of the breather ability to sustain long-lived oscillations of localized energy. Energy localization is an important phenomenon in a host of different physics disciplines from the formation of vortices in hydrodynamics to the self-focusing in optics or plasmas and from the formation of dislocations under stress in solids to the self-trapping of energy in proteins. Therefore there have been extensive studies not only of the application of similar techniques such as the ones used in the kink problems (as for example the variational approach encountered in [55]) but also of a number of other techniques .These methods can vary from map techniques used in chaotic dynamics to parallelize homoclinic and heteroclinic connections with localized lattice vibrations (see i.e. [56]-[57] ) to techniques of inverse scattering transformation perturbation theory yielding integrable limits of the equations under study(i.e. see [29]-[30]). Also given the analogy of the problem of localization of energy in the breather modes with the famous Anderson localization induced by disorder much attention has been drawn in the effort to localize energy in lattice systems due to non-linear effects as well as the existence of impurities. Hence many studies have focused to the study of breather-like impurities modeling linear lattices with non-linear impurities ([58]),as well to the non-thermal as well as thermalized interaction of the breathers with localized impurities ([59]) which can model for example the breaking of an H - bond between a base pair in a DNA molecule as occurs in realistic situations for $T << T_{denaturation}$.

Let us note in passing that even though our study will be (also for reasons of consistency) limited to the Sine-Gordon breathers the most studied equation in the context of breather modes is the Non-Linear Schrodinger equation. Its discrete version is given as :

$$i\dot{y} = -(y_{i+1} + y_{i-1}) - [\mu(y_{i+1} + y_{i-1}) + 2\nu y_n]|y_n|^2$$

One of the most striking results about this equation is the existence of an integrable limit called the Ablowitz-Ladik limit ([29]-[30]) (AL-NLS) which is simply : $i\dot{y_i}+(y_{i+1}+y_{i-1})(1+|y_i|)^2) = 0$ and which not only has an energy integral $H = \sum_i (y_i y^*_{i+1} + C.C.)$ and a momentum integral $P = i\sum_i (y_i y^*_{i+1} - C.C.)$ but also an infinite number of other invariants. In fact one can find an explicit expression for the discrete AL soliton $y_n = \sinh(b) sech(b(n-x)) \exp[ia(n-x) + i\sigma]$ where $\dot{x}, \dot{\sigma}$ are dependent on the constant parameters a,b according to the equations: $\dot{x} = \frac{2\sinh(b)\sin(a)}{b}$, $\dot{\sigma} = 2\cos(a)\cosh(b) + 2a\sinh(b)/b$ (see i.e. [62]) . For the very wide range of applications that this equation (NLS) has we will refer the interested reader to [63] (also a number of relevant applications is presented in the corresponding chapter of [12]).

In view of the extreme variety and richness of the problems arising in the study of breather-like excitations in non-linear Klein-Gordon lattices we will attempt to narrow our scope and try to answer some specific questions

concerning some issues raised in a number of recent publications. In particular we are going to address in our analytical and numerical studies the following questions:

- In a series of 3 papers ([59]-[61]) Peyrard and collaborators raised an important issue about the behavior of these localized excitations in the case of collisions. Their numerical findings for Klein-Gordon potentials of the form $V(y) = w_d^2(\frac{y_n^2}{2} - a\frac{y_n^3}{3} - b\frac{y_n^4}{4})$ seemed to indicate that (quoting [60]):"the world of discrete solitons is as merciless for the weak as the real world: in the presence of discreteness breather interactions show a systematic tendency to favor the growth of the larger excitation at the expense of the others". This ,if generically true , would be a very important statement because it would signify energy localization in a single very large excitation (which would subsequently be pinned by the P-N barrier and remain trapped thereafter). Thus we will pursue numerical studies of breather collisions in the F-K lattice comparing our results with [59]-[61].
- In another recent paper Cai et al. ([64]) have observed in the case of the NLS that for reflecting boundary conditions and for collisions of a breather with its image there is the possibility of trapping events in which the breather always returns to the 0th site travelling subsequently smaller and smaller spatial intervals and eventually is trapped on that site. Among parameter space regions (essentially initial velocity regions) for which this trapping resonance occurred there were noticed to exist escape windows for which the breather never returned (after the first collision) to the site 0. At the end of their paper these authors raise the question of whether the existence of such trapping resonances in the collision of localized excitations can be generically observed in Klein-Gordon lattices or whether it is a characteristic particular to the case of the NLS breather dynamics. We will therefore again translate the problem to the Sine-Gordon equation and will study the possibilities that occur in the parameter space of breather frequency .vs. initial velocity of the excitation.
- Finally we are going to show numerical simulations of the smallest possible breathing modes that can be statically (or dynamically) supported by lattices, namely, the Sievers-Takeno ([65]) and the Page ([66]) and we will present ,as an extension of the method presented for the 3 and 4 point kinks , the corresponding Evans function implementation in the case of 3 and 4 point breathers.

## 6.1 Breather Collisions

In our numerical study of breather interactions we always started with one breather with larger energy (and hence smaller frequency as well as larger amplitude) -typical values of its frequency were around $\simeq 0.1 - 0.2$ and one with less energy (bigger frequency -smaller amplitude) -typical values of frequency were in the range 0.4-0.5. Obviously the difference in energy between the 2 breathers is quite notable and hence if the results of Peyrard et. al. could be carried over to the case of the F-K lattice one should gradually observe through the many collisions between the 2 breathers in our periodic boundary condition domain that gradually the larger breather should be picking up energy from the smaller one.

The results of our numerical integrations (by means of a 4rth order R-K method) of the F-K lattice for the above mentioned discretized continuum breather initial conditions are shown in the figures [44]-[47]. We show a plot of the energy of the larger breather for a long time evolution run on the lattice (around 25000 time units with an integration step of 0.01 time units). The plot of $E_{larger}$ .vs. t shown corresponds to the lattice time evolution shown in the energy density contour plot - in both cases one can identify 8 collisional events. Also shown are details of individual collisions between the 2 breathers in terms of the outcome of them for the energy of the large breather. From these figures one can draw the following conclusions

1. The breathers are long-lived oscillatory and exponentially localized states that seem to persist for very long times moving along the lattice. Their energy is damped at a small rate and because of that they seem to persist even for very extended runs. Let us also note that in the contour plot shown the larger breather is shown to be moving. That was not the case in the original configurations (i.e. $v_{in} = 0$ for the larger breather). However as was also observed in [64] in the case of a non-integrable discrete system such the F-K model the soliton can acquire kinetic energy and move after the collision as opposed to case of the static soliton in integrable limits such as the AL-NLS equation (wherein the soliton is unable to move despite the collision)

2. The result of individual collisions between the breathers in the case of the discrete Sine-Gordon equation *cannot* be generically claimed to substantiate the conjecture that the collisions of large with smaller breathers result in energy pickup from the part of the larger breathers. In principle there seem to exist collisions in which the larger breather gains energy as well as others in which energy is gained by the smaller breather. On the average and closely observing the figure [44] one could claim that the larger breather has a gain of energy over long times but the behavior of individual collisions cannot be used as conclusive evidence that collisions always (or at least almost always as noted by Dauxois et al. in [60]) favor energetically the large energy breathers. One can clearly see a number of collisions, both in our detailed larger breather energy time evolution plots as well as in the contour plot indicating the breather collisions, that favor the larger breather as well as a number of others that favor the smaller one. On the basis of these results we believe that more numerical investigations are required in order to obtain a deeper understanding of the breather collisions in non-linear Klein-Gordon lattices.

## 6.2 Resonant Effects in Breather-Image Collisions

In [64] it was noted that for reflecting boundary conditions and collisions of a breather with its image (essentially through collision with the reflecting boundary and due to the symmetry of the configuration) that it is possible to obtain resonant structures. That is, it is possible to trap the incoming breather into a series of subsequent returns to the boundary site where it will eventually oscillate trapped in a form of a bound breather-image state. In the same paper the challenge of the necessity of similar investigations was posed in order to reveal the dynamics of breather-image collisions and to investigate whether such complex behavior is also realizable in the case of other non-linear K-G lattices.

Motivated by the above question we performed a series of numerical simulations in order to expose the dynamics of breather-image collisions in the parameter space of frequency .vs. velocity of the incoming breather for the F-K lattice. Our results are once again demonstrated in the form of a type of phase-diagram where the regimes are outlined (as can be seen in the figure [48]) .Exploring this phase diagram one can directly see that the breather-image dynamics presents an extreme wealth and diversity of possible behaviors (which we believe deserves further attention and many computational efforts in order to be understood in its full depth). We will attempt to touch upon these various potential outcomes of such collisions.

- For small value of the breather frequency ( i.e. $w < 0.3$ ) one always retrieves an outgoing breather(or rather 2 taking into consideration the symmetry of the problem under study) as a result of the collision. Of course the exact shape of the resulting breather is dependent on a delicate balance of the phase of the breather as well as its interaction with radiation effects and can vary significantly ; however the breather outcome of the collision seems to be quite robust (as a result) to the change of velocities in this range of frequencies. A typical time evolution of site zero (useful for comparison with the subsequently mentioned cases ) is given in figure [49] whereas a typical breather maximum space time plot is given in [50].
- For higher values of the frequency i.e. for $w \simeq 0.35$ in most of the cases under study an outgoing breather was the result of the simulation. However there was a small window of velocities (in the range of values $0.4 - 0.45$) for which the breather did return for a second collision with its image before escaping to infinity.A space time plot of the breather maximum in that regime is shown in [51]. This type of behavior prepared us for the quite unexpected events that occurred for even higher values of w (around 0.45). There apart from the regimes of velocities in which the outcome is an outgoing breather we found a window of velocities $(0.29 - 0.38)$ for which the result of the collision with image was a localized breathing oscillation at site 0 as well as an outgoing kink! Changing the sign of the initial condition and using the same delicate phase resonance one can also obtain an anti-kink. Initially, for v=0.29 one obtains a breather with short oscillation times and a kink (or an antikink) Even more to our surprise for higher values of the velocity (v=0.35) we found very long period oscillations and a kink propagating with a larger velocity whereas in contrast to that for v=0.38 (at the edge of the window of this behavior) we found a very fast propagating kink and even shorter period oscillations than at $v = 0.29$. These results are demonstrated graphically in the space-time plot of figure [52], in the site zero time evolution graphs [53]-[54] and in the 3d representation [$3d_6$] (again for the case of $v = 0.29$).

- Investigating the regime of frequencies between the 2 above mentioned cases (i.e. w=0.4) we were able to trace another regime of parameters (a very narrow one in fact- w=0.4 , $v \simeq 0.55$) for which we finally managed to observe a resonance similar to the one mentioned by Cai et al. to occur in the F-K lattice. This phenomenon (shown in the space time plots of the figures [55]-[57]) exhibited a number of continuous returns of the breather at the 0th site finally resulting in a trapping oscillation of it centered at that site. Let us note that this was a very delicate phenomenon since at v=0.555 for the same frequency we got a number of returns but eventually the breather managed to escape , whereas just before this velocity (at v=0.545 ) the result of the collision is again a kink rather than a trapped breather.

The above indicate that the various regimes of parameters (and also d which in our study was for simplicity set to 1.0 but which obviously is another parameter strongly affecting the dynamics) show a very rich structural behavior which should be addressed more carefully. We will, however, leave this endeavor for future studies.

### 6.3 3 and 4 Point Breathers

The last question that we would like to address concerns the stability issues of these intrinsic localised modes. For reasons of simplicity we are going to limit our study to the stability of 3 and 4 point breathers that have received much attention over the past decade in the bibliography.

In a pioneering paper on the 3 point breathing excitation that now bears their name Sievers and Takeno ([65]) introduced the 3 point breather excitation which consists of the configuration : $A(0,...,0,-1/2,1,-1/2,0,...,0)\exp(iwt)$. This pattern has been found in the original paper S-T to have a frequency of $w^2 = 3(k_2 + \frac{27}{16}k_4A^2)$. A in this expression is the mode amplitude $k_2$ is the coefficient of the quadratic non-linearity and $k_4$ the one of the quartic. For this particular problem, as is usually done in the bibliography, we will limit ourselves to potentials of the form $V = \frac{k_2}{2}(y_{i+1} - y_i)^2 + \frac{k_4}{4}(y_{i+1} - y_i)^4$ (even though as is shown in [65] the results are almost exact solutions for higher order non-linearities in the potential).

In the original S-T paper the method used in order to obtain the above solution was the 1d harmonic lattice Green's functions technique. Using this technique they were also able to detect that this odd parity localised mode should be stable for $\lambda = \frac{k_4A^2}{k_2} >> 16/81$.

Page ([66]) was the first to appreciate the significance of the S-T findings. He studied the same problem within the context of the rotating wave approximation and was able to trace not only the odd parity modes of S-T but also even parity modes (the Page mode) that has been proved to be much more stable the S-T pattern. The essence of the RWA approach lies in the substitution of the ansatz $y_n = Au_n\cos(wt)$ in the equations of motion $\ddot{y_n} = \frac{\partial V}{\partial y_n}$ in the above potential. In the resulting equation apart from the terms $\propto \cos(wt)$ there are also terms $\propto \cos^3(wt)$. Within the context of this approximation one keeps in the expression (or in general for higher order anharmonicities of the expression $\propto \cos(wt)^{r-1}$) only the terms that are proportional to $\cos(wt)$ according to the analysis:

$$\cos(wt)^{r-1} = C_r\cos(wt) + higher \qquad harmonics$$

where $C_r = \frac{(r-1)}{2^{r-2}(r/2)(r/2-1)}$. Then one can find the even pattern

$$A(0,...,0,-1/6,1,-1,1/6,0,...,0)\exp(iwt)$$

with the frequency $w^2 = 3A^2(k_2 + 2k_4[1 + (\frac{7}{12})^3])$ which has been proved to be very robustly stable to perturbations in previous numerical simulations.Our numerical experiments have revealed the possibility of existence and localised oscillation of these modes in quadratic plus quartic lattice for the Page mode and in purely quartic for the S-T mode as is shown in the figures [58]-[59].

The first attempt to explore the stability of these modes was given in a subsequent paper by Page and collaborators ([67]) wherein they consider solutions of the equations of the functional form : $y_n = Au_n\cos(wt + \phi_n)$. This choice of ansatz motivated by studies of stability in problems related to the phase and amplitude turbulence exhibited in the Complex Ginzburg Landau equation (CGL) allows for time and site dependent phase modulation. Considering that modulation to be relatively small the above authors used the formula: $\cos(wt + \phi_{n\pm1}) \simeq \cos(wt + \phi_n) - \sin(wt + \phi_n)(\phi_{n\pm1} - \phi_n)$ along with RWA (or an equivalent averaging over a period of the resulting

equations after multiplication with the sine and the cosine $(wt + \phi_n)$ term to obtain 2 second order coupled ODE's for $\phi_n, u_n$ (equations 11,12 of [67]). Then analyzing the amplitude and phase part to its corresponding steady state (S-T or Page mode) plus perturbations they were able to do ODE stability analysis finding good agreement with numerical simulations and concluding that:

- The Page mode is very stable under perturbations
- The S-T mode is unstable in the case of quadratic plus quartic lattice yielding according to the amplitude of the perturbation imposed either a travelling localized mode or a static Page mode or one that oscillates between adjacent sites.

In order to verify their results we used the Evans function technique for the detection of potential instabilities in the S-T and Page modes.Let us illustrate the method's application in the case of the S-T mode and then we will give only the results for the case of the Page mode.
We will use the ansatz $y_n = u_n + v_n \exp((\lambda + iw)t)$ in the harmonic plus quartic case in which the pattern will be considered to be exact (which as is well known is a very good approximation) and we will find the potential instabilities to arise as zeros of the corresponding Evans functions for the perturbation $v_n$. Thus using the fact that $u_n$ is a solution to the equation $\ddot{y_n} = -\frac{\partial V}{\partial y_n}$ and substituting the ansatz we obtain an equation for $v_n$:

$$(\lambda + iw)^2 v_n = k_2(v_{n+1} + v_{n-1} - 2v_n) + 3A^2 k_4 \cos^3(wt)(u_{n+1} - u_n)^2(v_{n+1} - v_n)$$
$$+3k_4 A^2 \cos^3(wt)(u_{n-1} - u_n)^2(v_{n-1} - v_n)$$

Since our intention is to create the Nyquist plots of $D(i\lambda)$ we will hereafter incorporate $\lambda + w = l$ and also we will apply once again the RWA $\cos^3(wt) = (3/4)cos(wt)$ + higher harmonics. Using for simplicity the terminology $s = -l^2/k_2$, $a = \frac{9k_4A^2}{4k_2}$ we then obtain that the solutions $v_n$ to the far ends will be $\propto Ar^n + B{r_1}^n$ where $r, r_1 = \frac{s+2+\sqrt{(s(s+4))}}{2}$ (r is considered to be the one with $|r| > 1$ whereas $|r_1| < 1$). Then one, starting on the left far end with a solution of the form $r^n$ which is decaying at $-\infty$, can propagate it on the lattice, using the far end equation, down to $v_{-2} = r^{-2}$ as an outcome of the equation of $v_{-3} = r^{-3}$. Then as one goes to the equation for the site -2 one has to take into consideration the non-zero contribution of the breather. Thus one has to "shoot" the solution through the 3 point S-T breather. This can be done by solving the corresponding equations for the sites (-2,-1,0,1,2). Straightforward algebraic manipulations then yield:
$v_{-1} = -(a_{11}/r^2 + 1/r^3)/a_{12}$
$v_0 = -(a_{12}/r^2 + a_{22}v_{-1})/a_{23}$
$v_1 = -(a_{23}v_{-1} + a_{33}v_0)/a_{23}$
$v_2 = -(a_{23}v_0 + a_{33}v_1)/a_{12}$
$v_3 = -(a_{12}v_1 + a_{11}v_2)$
Then using the fact, once again, that according to the Evans prescription $v_2 = Ar^2 + B{r_1}^2$, $v_3 = Ar^3 + B{r_1}^3$ we can derive the equation for the evans function $D(i\lambda) = {r_1}^3(r_1v_2 - v_3)$ normalizing appropriately after elimination of the poles introduced by the factor $r_1 - r$. The matrix elements are $a_{11} = -s - 2 - (1/4)a$ , $a_{22} = -s - 2 - (10/4)a$, $a_{33} = -s - 2 - (9/2)a$, $a_{12} = 1 + (1/4)a$, $a_{23} == 1 + (9/4)a$.

In the case of the Page mode the manipulations are exactly the same with propagation of the far end equation down to the site -3 (i.e. $v_{-3} = r^{-3}$) .Then shooting through the Page breather we find:
$v_{-2} = -(a_{11}/r^3 + 1/r^4)/a_{12}$
$v_{-1} = -(a_{12}/r^3 + a_{22}v_{-2})/a_{23}$
$v_0 = -(a_{23}v_{-2} + a_{33}v_{-1})/a_{34}$
$v_1 = -(a_{34}v_{-1} + a_{33}v_0)/a_{23}$
$v_2 = -(a_{23}v_0 + a_{11}v_1)/a_{12}$
$v_3 = -(a_{12}v_1 + a_{11}v_2)$
and thus $D(i\lambda) = ({r_1}^3)(r_1v_2 - v_3)$ where the matrix elements now are: $a_{11} = -s - 2 - (1/36)a$, $a_{22} = -s - 2 - (50/36)a$, $a_{33} = -s - 2 - (4 + (49/36))a$, $a_{12} = 1 + (1/36)a$, $a_{23} = 1 + (49/36)a$,$a_{34} = 1 + 4a$.

Preliminary numerical investigations demonstrate that in the case of the Page mode there are no enclosures in the Nyquist plot of the Evans function and thus it is a stable mode as was originally conjectured by Page by means of

numerical observations and subsequently substantiated by Sandusky , Page and Schmidt by means of the eigenvalue analysis mentioned above. On the other hand the Nyquist plot of the Evans function for the S-T mode shows a number of enclosures that verify the result of [67] that it should be highly unstable to perturbations in the quadratic plus quartic case.

This analysis of the stability of the smallest possible breather modes introduces the possibility of application of the Evans function technique for the study of breathers.This type of analysis can be extended in a straightforward way for any soliton-like excitation (as we have seen for example also in the case of kinks) on the lattice yielding a very natural ground for the application of this technique for stability studies (since the differential equations are reduced to matrix equations which can be easily solved analytically -as was done for simple cases here- or numerically).

This subsection concludes our short excursion to the world of solitonic excitations of the kink and breather form. In the last paragraph of this work we will summarize our findings and illustrate some of the potential challenges for future work.

# 7 Conclusions & Future Challenges

As we have seen in this paper the picture of solitons that has been well established over the last decades for the continuum models that have been used in many physical applications(i.e. Sine-Gordon , $\phi^4$, Non-Linear Schrodinger) is drastically different on discrete lattices. On many of the applications of the solitonic excitations (DNA, Dislocations) the discrete nature of the problem necessitates a deeper and more quantitative understanding of the intrinsically discrete characteristics of the problem.

These main ones among these characteristics are:

- The Peierls-Nabarro barrier in which the kink and/or breather solutions have to move and which can cause them to get pinned.
- The birth of intrinsic localised shape modes of the kinks which are absent in the continuum case.
- The emission of radiation due to resonance phenomena of either the kink characteristic frequency (when the kink is in motion) or of the Peierls-Nabarro frequency (when the kink is pinned at later stages of its time evolution) with the frequencies of the phonon spectrum.
- The Brownian motion of the kink as driven by the fluctuations (superposed to the dissipative process of kink energy loss due to radiative phenomena)
- The creation of stable and unstable configurations in the P-N barrier which can be traced by the method of the Evans functions (in the continuum all kink-like configurations are energytically equivalent due to translational invariance)
- The appearance of new phenomena in the kink-kink as well as kink-antikink collisions which appear to have a much richer behavior than their continuum counterpart and whose theoretical understanding is far from being complete.
- The existence and propagation on the lattice of "higher order" kinks which despite the fact that they are not exact solutions of the equations of motion, can still propagate through the lattice at higher velocities and with very small radiation in their wake.We have given the pinning - depinning transition phase diagram for these higher amplitude modes and have sketched its analogies with other transitions of this form (i.e. fluid mechanical ones).

All the above have led us to the understanding that conventional discretizations introduce new (and non-existent in the continuum) phenomena in the continuum models and thus we have presented and applied a method for constructing efficient alternative numerical algorithms in which some of these phenomena (such as the P-N barrier) are not present.

We have also extended our study to the discrete Sine-Gordon breathers where we have revealed that collisional outcomes do not necessarily favor the growth of the larger energy breather as had been claimed in the bibliography.

Also we have presented numerical evidence for a host of new and interesting phenomena arising from collisions of breathers and their images through reflecting boudaries. Finally we have outlined the application of Evans function techniques for the case of the smallest possible breathing modes , namely the Sievers-Takeno and the Page mode, This technique, as is indicated by our applications both for the 3,4 point kinks and for the S-T and Page breathers, seems to be ideally suited for stability studies of solitonic excitations (as well as localised excitations more generally ) in discrete lattices.

A direct and very challenging question that naturally arises from this study concerns the theoretical understanding of interactions between discrete solitons. The single kink or breather behavior on a discrete lattice seems to be by now well understood and the numerical experiments along with the theoretical explanations of our work give an overview of this picture. However as seen above the collisional outcomes of the soiton-soliton as well as of soliton-antisoliton interactions are extremely complex and to date there is no simple model that can comprehensively incorporate these characteristics (the BWS theory is an interesting and useful theory but it still requires the solution of a cumbersome -in fact much more cumbersome than the original system of ,say, 402 coupled ordinary differential equations !). This appears to be a very interesting (as well as difficult) theoretical problem. Moreover as demonstrated by our simulations also the multibreather systems appear to demonstrate a number of interesting collisional possibilities (as was originally found to be the case in the NLS equation). Undoubtedly a deeper understanding of this dynamics could shed more light to the (important to many practical applications) problem of energy localisation in non-linear lattices.

Finally, further possible extensions that are currently being explored are the generalisations of these phenomena in 2 and 3 dimensional problems in which these models (that can be used for example as models of coupled mass and charge transport in systems with strong interactomic interactions)also appear to demonstrate some new physics (i.e. see [68]-[70]).An example of this form is the non-linear mobility and the corresponding hysteresis curves in mobility .vs. applied force in 2 dimensional F-K chains. Another potentially interesting application could lie on the study of coupled F-K lattices (by diffusional coupling or otherwise). Some preliminary studies of the subject ([71]) have revealed new possible modes such as the so-called "bi-soliton mode".

Therefore we believe that the subject of solitonic excitations in discrete lattices deserves further attention and many possibilities for analytical and numerical investigations arise from the numerous and challenging questions that the subject poses. We believe that a lot of interesting new physics is yet to be unveiled in the subject which will be quite relevant to a host of different applications.

**Acknowledgments:** The author would like to thank Dr. N.J. Balmforth and Dr. P.J. Morrison for their help and guidance during this work. This work has been supported by the Geophysical Fluid Dynamics Fellowship of the Woods Hole Oceanographic Institution.

# References

[1] N.J. Zabusky and M.D. Kruskal *Phys. Rev. Letters* ,**15**, 240, 1965

[2] N.J. Zabusky , G.S. Deem , M.D. Kruskal , Formation , Propagation and Interaction of Solitons 16mm Cine Film

[3] D.W. McLaughlin , A.C. Scott *Phys Rev. A* , **18**, 4 , 1652, 1978

[4] W.P. Su and J.R. Schrieffer *Phys. Rev. Letters* , **46** ,11 ,738 ,1981

[5] A.R. Bishop , S.E. Trullinger and J.A. Krumhansl *Physica D* , **1** ,1 ,1980

[6] J.F. Curie , S.E. Trullinger A.R. Bishop and J.A. Krumhansl *Phys. Rev. B* , **15** ,5567 ,1976

[7] M. Peyrard and A.R. Bishop *Phys. Rev. Letters* , **62** ,23 ,2755 ,1989

[8] T. Dauxois,M. Peyrard and A.R. Bishop *Phys. Rev. E* , **47** ,R 44 ,1993

[9] T. Dauxois, M. Peyrard and A.R. Bishop *Phys. Rev. E* , **47** ,1 ,684, 1993

[10] A.R. Bishop and T.F. Lewis *J. Phys. C* , **12** ,3811 , 1979

[11] J. Krumhansl and J.R. Scrhieffer *Phys. Rev. B* , **11** ,3535 ,1975

[12] R.K. Dodd, J.C. Eilbeck, J.D. Gibbon and H.C. Morris Solitons and Non-Linear Wave Equations Academic Press, London , 1982

[13] P.J. Morrison *Rev. Mod. Physics* , **70** ,2 ,467, 1998

[14] J. Frenkel and T. Kontorova *J. Phys.* , **1** ,137 ,1939

[15] M. Peyrard and M.D. Kruskal *Physica D* , **14** ,88 ,1984

[16] P. Stancioff , C. Willis, M. El-Batanouny and S. Burdick *Phys. Rev. B* , **33** ,3 ,1912, 1986

[17] C. Willis , M. El-Batanouny and P. Stancioff *Phys. Rev. B* , **33** ,3 ,1904 ,1986

[18] R. Boesch, C.R. Willis and M. El-Batanouny *Phys. Rev. B* , **40** ,4 , 2284, 1989

[19] R. Boesch, P. Stancioff and C.R. Willis *Phys. Rev. B* , **38** ,10 ,6713, 1988

[20] R. Boesch and C.R. Willis *Phys. Rev. B* , **39** ,1 ,361 , 1989

[21] C.R. Willis and R. Boesch *Phys. Rev. B* , **41** ,7 ,4570 , 1990

[22] R. Boesch and C.R. Willis *Phys. Rev. B* , **42** ,10 , 6371, 1990

[23] R. Ravelo , M. El-Batanouny, C.R.Willis and P.Sodano *Phys. Rev. B* , **38** ,7 ,4817, 1988

[24] E. Tomboulis *Phys. Rev. D* , **12** ,1678 ,1975

[25] J.A. Combs and S. Yip *Phys. Rev. B* , **28** ,12 ,6873 , 1983

[26] Y. Ishimori and T. Munakata *J. Phys. Soc. Japan* , **51** ,3367 ,1982

[27] J.P. Keener and D.W. McLaughlin *Phys. Rev. A* , **16** ,777 ,1977

[28] Yu.S. Kivshar and D.K. Campbell *Phys. Rev. E* , **48** ,4 ,3077, 1993

[29] M. Ablowitz and J. Ladik *J. Math. Phys.* , **16** ,598 ,1975

[30] M. Ablowitz and J. Ladik *J. Math. Phys* , **17** ,6 ,1010, 1976

[31] J.A. Combs and S. Yip *Phys. Rev. B* , **29** ,438 ,1984

[32] C.R. Willis and M. El-Batanouny (unpublished)

[33] P.S. Sahni and G.F. Mazenko *Phys. Rev. B* , **20** , 4674 , 1979

[34] O.M. Braun, Yu.S. Kivshar and M. Peyrard *Phys. Rev. E* , **56** ,5 ,6050, 1997

[35] M. Peyrard and M. Ramoissenet *Phys. Rev. B* , **26** ,2886 ,1982

[36] J. Evans *Indiana Univ. Math. J.* , **24** ,1169 ,1975

[37] J. Alexander , R. Gardner and C.K.R. Jones *J. Reine Angew. Math,* , **410** ,167 ,1990

[38] R.L. Pego, P. Smereka and W.I. Weinstein *Physica D* , **67** ,45 ,1993

[39] R.L. Pego and W.I. Weinstein *Phil. Trans Roy. Soc. A* , **340** ,47 ,1993

[40] N.J. Balmforth, R.V. Craster and S.J.A.Malham (preprint)

[41] D.K. Campbell , J.F.Schonfeld and C.A. Wingate *Physica D* , **9** ,1 ,1983

[42] Yu. S. Kivshar, D.E. Pelinovsky , T. Cretegny and M. Peyrard *Phys. Rev. Letters* , **80** ,23 ,5032 , 1998

[43] R. Boesch and M. Peyrard *Phys. Rev. B* , **43** ,10 ,8491 , 1991

[44] Y. Hsu *Phys. Rev. B* , **22** ,6 ,1394, 1978

[45] A.L. Barabasi and H.E. Stanley Fractal Concepts in Surface Growth Cambridge University Press, 1995

[46] N. Martys , M. Cieplak and M.O. Robbins *Phys. Rev. Letters* , **66** ,1058 , 1991

[47] M. Peyrard and S. Aubry *J. Phys. C* , **16** ,1593 ,1983

[48] E.B. Bogomol'nyi *Sov. J. Nuc. Phys.* , **24** ,449 ,1976

[49] J.M. Speight and R.S. Ward *Nonlinearity* , **7** ,475 ,1994

[50] J.M. Speight *Nonlinearity* , **10** ,1615 ,1997

[51] W.J. Zakrzewski *Nonlinearity* , **8** ,517 , 1995

[52] E. Majernikova *Phys. Rev. E* , **49** ,3360 ,1994

[53] R.S. MacKay and S. Aubry *Nonlinearity* , **7** ,1623 ,1994

[54] J.L. Marin and S. Aubry *Nonlinearity* , **9** ,1501 ,1996

[55] J.D. Wattis *Nonlinearity* , **9** ,1583 ,1996

[56] S. Flash , C.R. Willis and E. Olbrich *Phys. Rev. E* , **49** ,1 ,836, 1994

[57] D. Hennig , K.O. Rasmussen,H. Gabriel and A. Bulow *Phys. Rev. E* , **54** ,5 , 5788, 1996

[58] D. Hennig, K.O.Rasmussen, G.P. Tsironis and H. Gabriel *Phys. Rev. E* , **52** , 5 ,R 4628, 1995

[59] T. Dauxois,M. Peyrard and C.R. Willis *Phys. Rev. E* , **48** ,6 ,4768, 1993

[60] T. Dauxois and M. Peyrard *Phys. Rev. Letters* , **70** ,25 ,1993

[61] O. Bang and M. Peyrard *Phys. Rev. E* , **53** ,4 ,1996

[62] D. Cai , A.R. Bishop and N. Gronbech-Jensen *Phys. Rev. E* , **53** ,4 , 4131 ,1996

[63] P.L. Christiansen, J.C. Eilbeck and R.D. Parmentier *Physica D* , **68** ,1 , 1993

[64] D. Cai, A.R. Bishop and N. Gronbech-Jensen *Phys. Rev. E* , **56** ,6 ,7246, 1997

[65] A.J. Sievers and S. Takeno *Phys. Rev. Letters* , **61** ,8 ,970 ,1988

[66] J.B. Page *Phys. Rev. B* , **41** ,11 ,7835, 1990

[67] K.W. Sandusky, J.B. Page and K.E. Schmidt *Phys. Rev. B* , **46** ,10 ,6161, 1992

[68] O.M. Braun , T. Dauxois , M.V. Paliy and M. Peyrard *Phys. Rev. E* , **55** ,3 ,3598, 1997

[69] O.M. Braun , T. Dauxois , M.V. Paliy and M. Peyrard *Phys. Rev. Letters* , **78** ,7 ,1295, 1997

[70] T. Strunz and F.J. Elmer (preprint)

[71] P Woafo *Phys. Rev. B* , **52** ,9 , 6170, 1995

## Captions of 3d Plots

[$3d_1$] :Propagating 2 $\pi$ Kink in the F-K Lattice
[$3d_2$] : k-k Pair Collision for d=1.15 , $v_{smaller} = 0.1$
[$3d_3$] : k-$\bar{k}$ Collision for d=1.0 , $v_{\bar{k}} = 0.8$
[$3d_4$] : k-$\bar{k}$ Collision for d=1.0 , $v_{\bar{k}} = 0.1$: Breather Formation, Propagation and Direction Reversal

[$3d_5$] : Kink Propagating in the Modified (by Speight) $\phi^4$ Without Feeling a P-N Barrier, $v_0 = 0.35$: almost no radiation!
[$3d_6$] : Evolution of Breather Image Collision to an Outgoing Kink : d=1.0, v=0.29, w=0.45

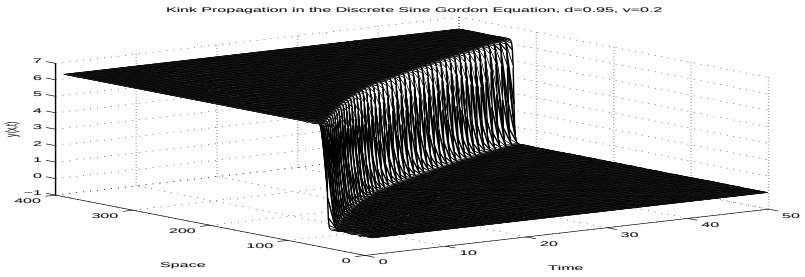


Figure 61: 3d Plots: Figure [$3d_1$]

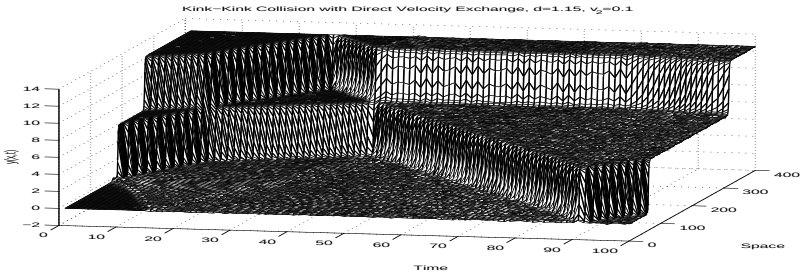


Figure 62: 3d Plots: Figure [$3d_2$]

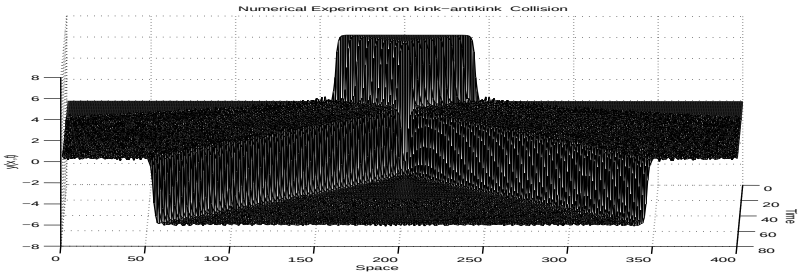


Figure 63: 3d Plots: Figure [$3d_3$]

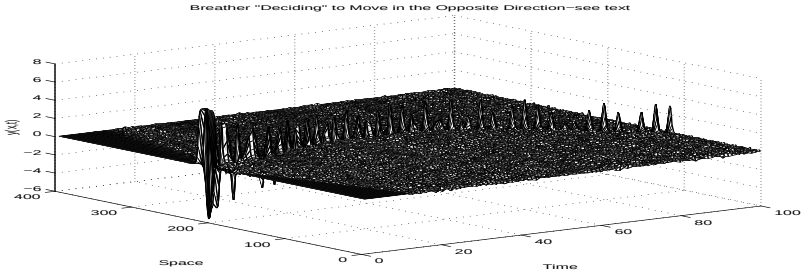


Figure 64: 3d Plots: Figure [$3d_4$]

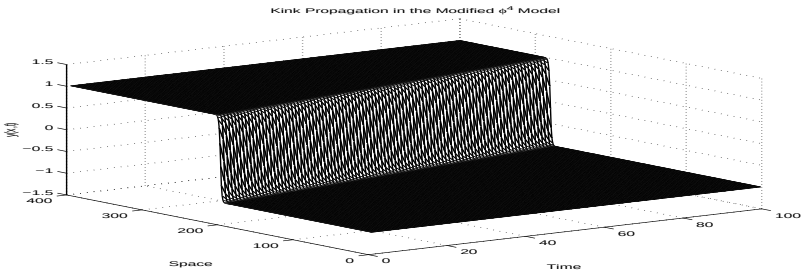


Figure 65: 3d Plots: Figure [$3d_5$]

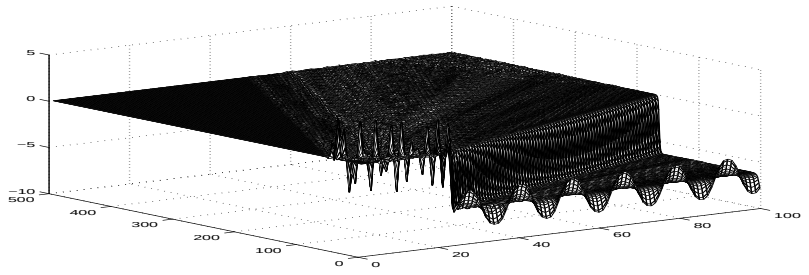


Figure 66: 3d Plots: Figure [$3d_6$]